

Galactic cosmic rays and the role of precision cross-sections

Fiorenza Donato
Torino University & INFN & CERN

LAPP - Annecy-le-Vieux 23/05/2025

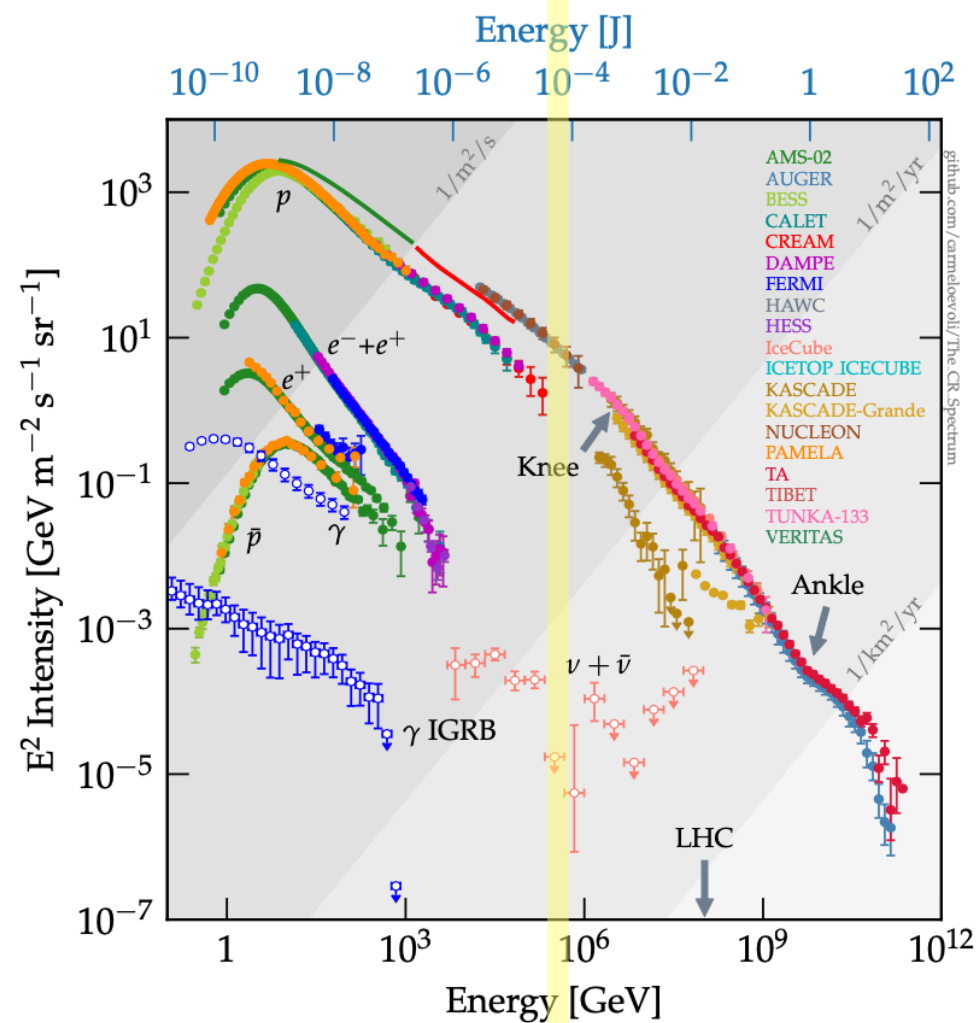
Structure of the seminar

- Introduction of Galactic Cosmic Rays (GCR)
- The physics cases for cross sections (XS)
- Cross sections needs for GCRs: state of the art and sought precision
- Main facilities to perform XS experiments (CERN mainly)

GALACTIC COSMIC RAYS

are charged particles (nuclei, isotopes, leptons, antiparticles)
diffusing in the galactic magnetic field
Observed at Earth with $E \sim 10 \text{ MeV/n} - 10^3 \text{ TeV/n}$

Gabici, Evoli, Gaggero, Lipari, Mertsch,
Orlando, Strong, Vittino 1903.11584



Direct detection
(circa Galactic)

Indirect

CR database: D. Maurin+ EPJC 2023

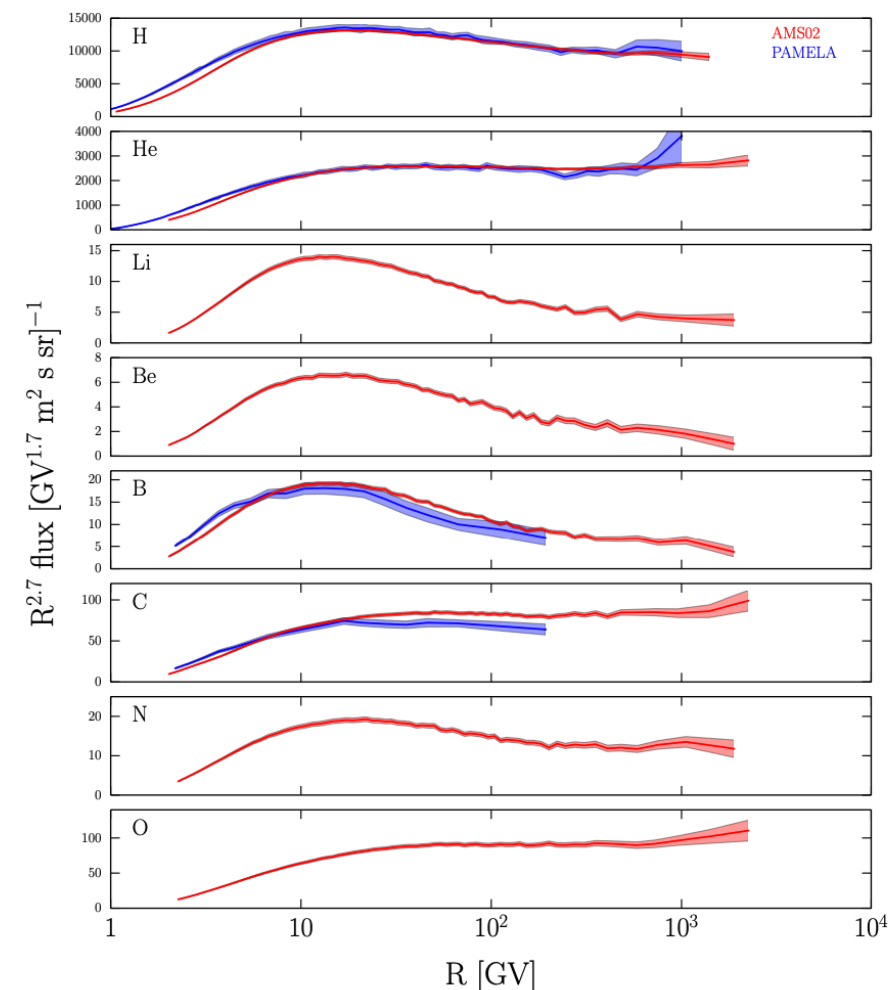
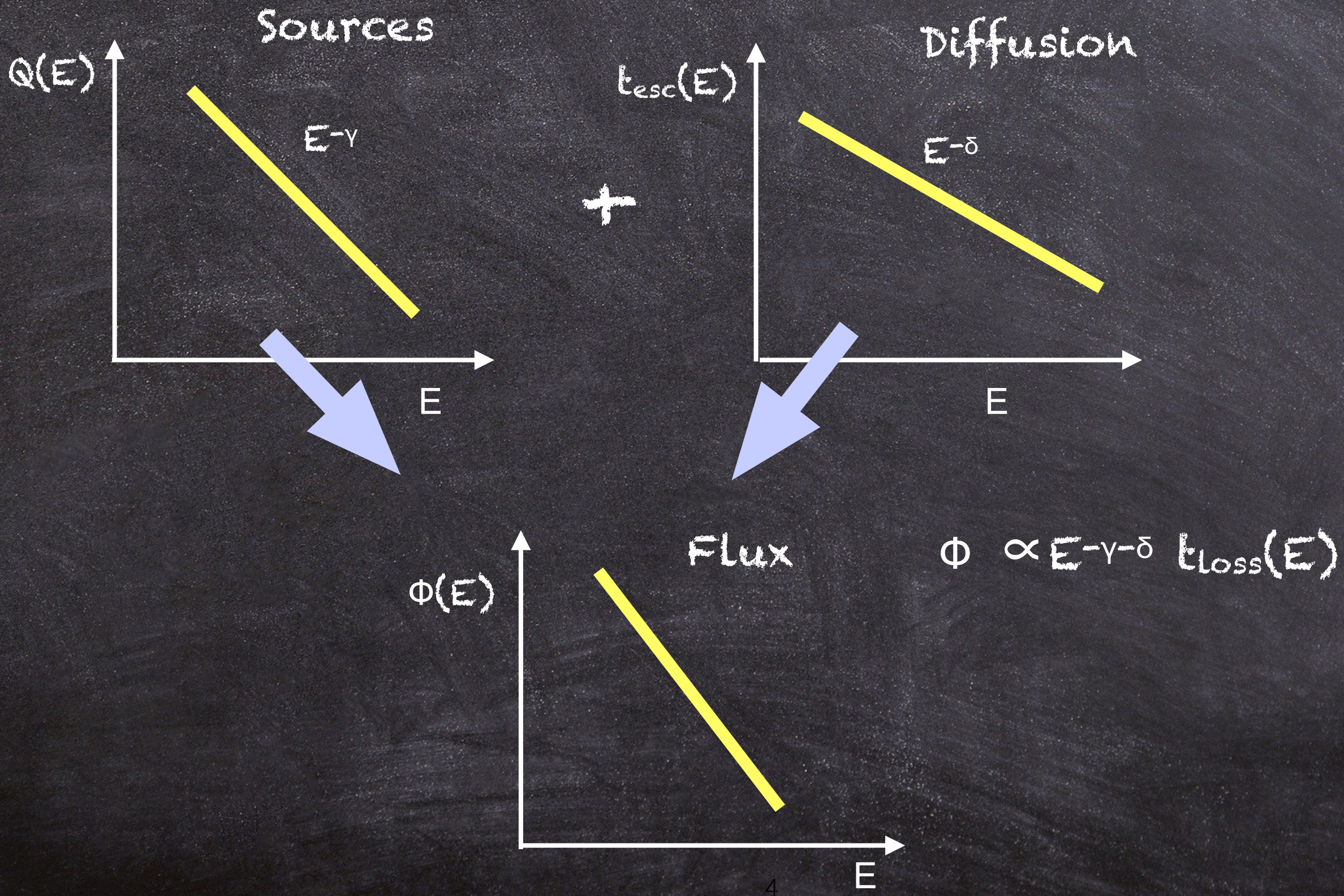


Fig. 1. The individual CR flux for nuclear species up to Oxygen as measured by PAMELA and AMS02. Shadow regions correspond to 1 sigma total errors (systematic and statistical added in quadrature).

CRs at zero-th order

or: In the old times there were power laws



1. The bulk of the energy of CRs comes from SNR explosions in the galactic disk

The power of \sim GeV CRs can be computed (Strong+ApJL 2010) from γ rays as $P_{CR} \sim 10^{41}$ erg/s. It is equivalent to the power of observed SuperNova Remnants (SNRs) in the Galaxy

2. CRs are accelerated through diffusive shock acceleration in SNRs

SNRs provide the right energy needed for CRs (Baade&Zwicky 1934)

Classical test is through γ -rays observations of SNRs (O'Drury+ A&A1994)

Still some ambiguities on hadron acceleration by SNRs which, could be explained by leptonic emission (i.e. SNR RX J1713.7-3946)

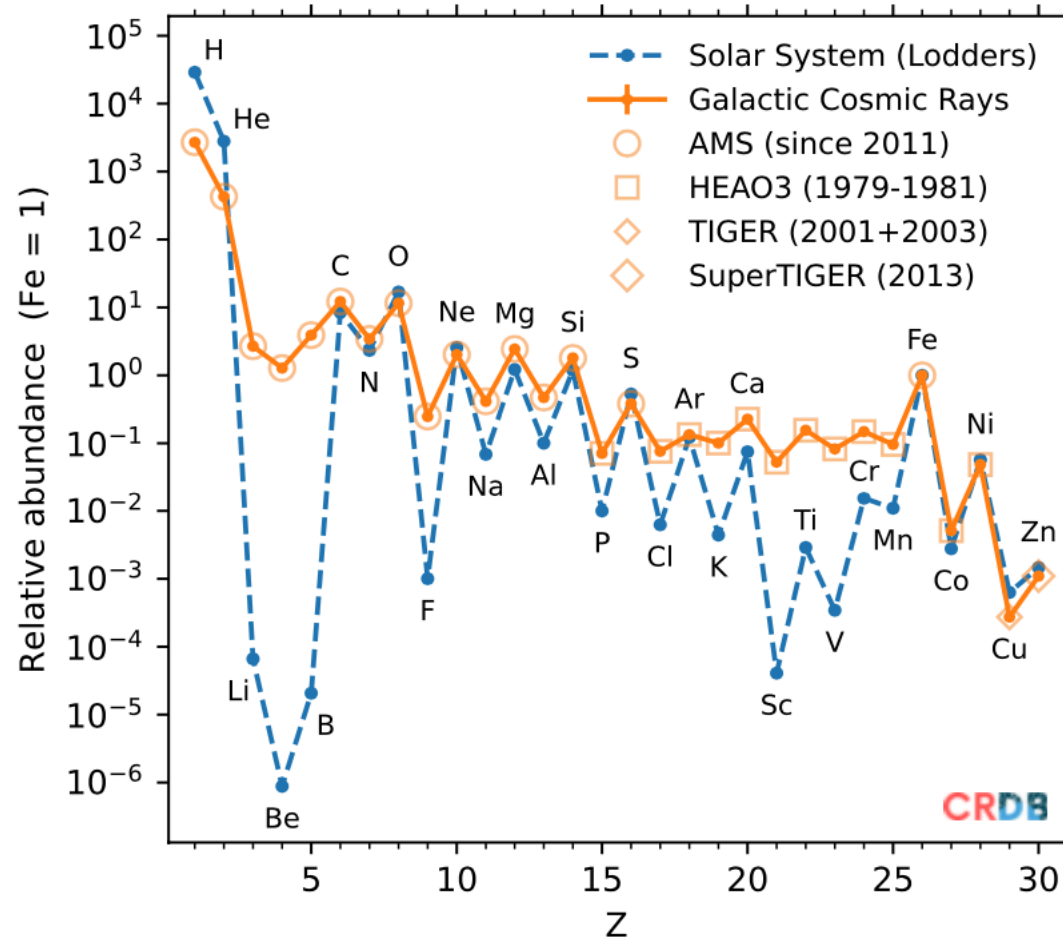
See Bell MNRAS 1978, MNRAS2004, Bell+MNRAS2013; Caprioli+ MNRAS2009; Blasi+ApJ2012 ; Recchia&Gabici MNRAS2018

Probe: detection of the maximum energy at 67.5 MeV in the π^0 decay rest frame;
 γ rays from molecular clouds illuminated by nearby, freshly accelerated protons

3. Composition: primary, secondaries, both

Primaries: produced in the sources (SNR and Pulsars): H, He, CNO, Fe; e^- , e^+ ; possibly e^+ , p^- , d^- from Dark Matter annihilation/decay

Secondaries: produced by spallation of primary CRs (p, He, C, O, Fe) on the interstellar medium (ISM): Li, Be, B, sub-Fe, [...], (radioactive) isotopes ; e^+ , p^- , d^-



Solar System abundances are deprived of nuclei such as Li, Be, B, sub-Fe, likely of secondary origin

All species are, at some extent, both primaries and secondaries

4. CRs are diffusively confined in an extended magnetic halo

CRs must be confined a region much thicker than the Galactic disk. Radioactive isotopes such as ^{10}Be indicate the existence of a magnetic diffusive halo several kpc thick (L or H)

$$D(R) \sim D_0 \times f(R) \sim D_0 \times R^\delta$$

$$D_0 \sim 3 \times 10^{28} \left(\frac{H}{5 \text{ kpc}} \right) \left(\frac{\Lambda}{10 \text{ g/cm}^2} \right)^{-1} \text{ cm}^2/\text{s} .$$

Radio haloes observed in external galaxies.

A very extended halo, $> 100 \text{ kpc}$, has been observed across **M31** (Karwin+ ApJ2019).

DM annihilation has been explored (Karwin+2020).

Non-standard propagation of CRs can explain it (Recchia+ ApJ2021)

Propagation equation

$$\frac{\partial \psi_i(\mathbf{x}, p, t)}{\partial t} = q_i(\mathbf{x}, p) + \nabla \cdot (D_{xx} \nabla \psi_i - \mathbf{V} \psi_i) \\ + \frac{\partial}{\partial p} p^2 D_{pp} \frac{\partial}{\partial p} \frac{1}{p^2} \psi_i - \frac{\partial}{\partial p} \left(\frac{dp}{dt} \psi_i - \frac{p}{3} (\nabla \cdot \mathbf{V}) \psi_i \right) - \frac{1}{\tau_{f,i}} \psi_i - \frac{1}{\tau_{r,i}} \psi_i.$$

Diffusion: $D(\mathbf{x}, R)$ a priori

usually assumed isotropic in the Galaxy: $D(R) = D_0 R^\delta$ ($R = pc/Ze$)
 D_0 and δ preferably fixed by B/C (Kappl+15; Genolini+15 (K15))

Sources: injection from stellar relics (SNRs, PWN)

Spallation from nuclei scattering off the interstellar medium (ISM)

Energy losses: Nuclei: ionisation, Coulomb (spallations)

Leptons: Synchrotron on the galactic $B \sim 3 \mu\text{G}$

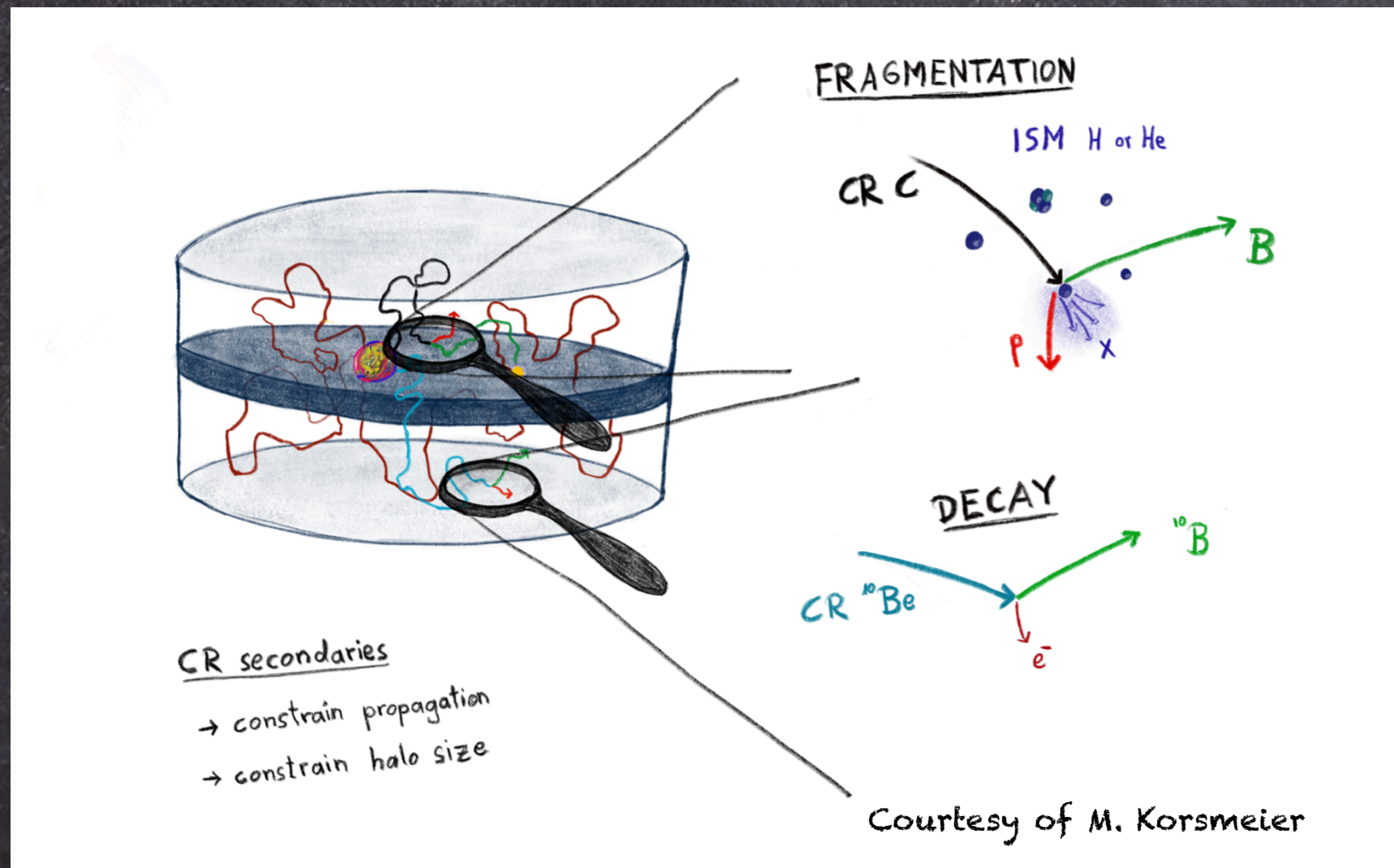
Inverse Compton on photon fields (stellar, CMB, UV, IR)

Geometry of the Galaxy: cylinder with half-height $L \sim \text{kpc}$

Solution of the eq.: semi-analytic (Maurin+ 2001, Donato+ 2004, Maurin 2018 ...), USINE codes
or fully numerical: GALPROP (Strong & Moskalenko 1998), DRAGON (Evoli+ 2008; 2016), PICARD
(Kissmann, 2014, Kissmann+ 2015)

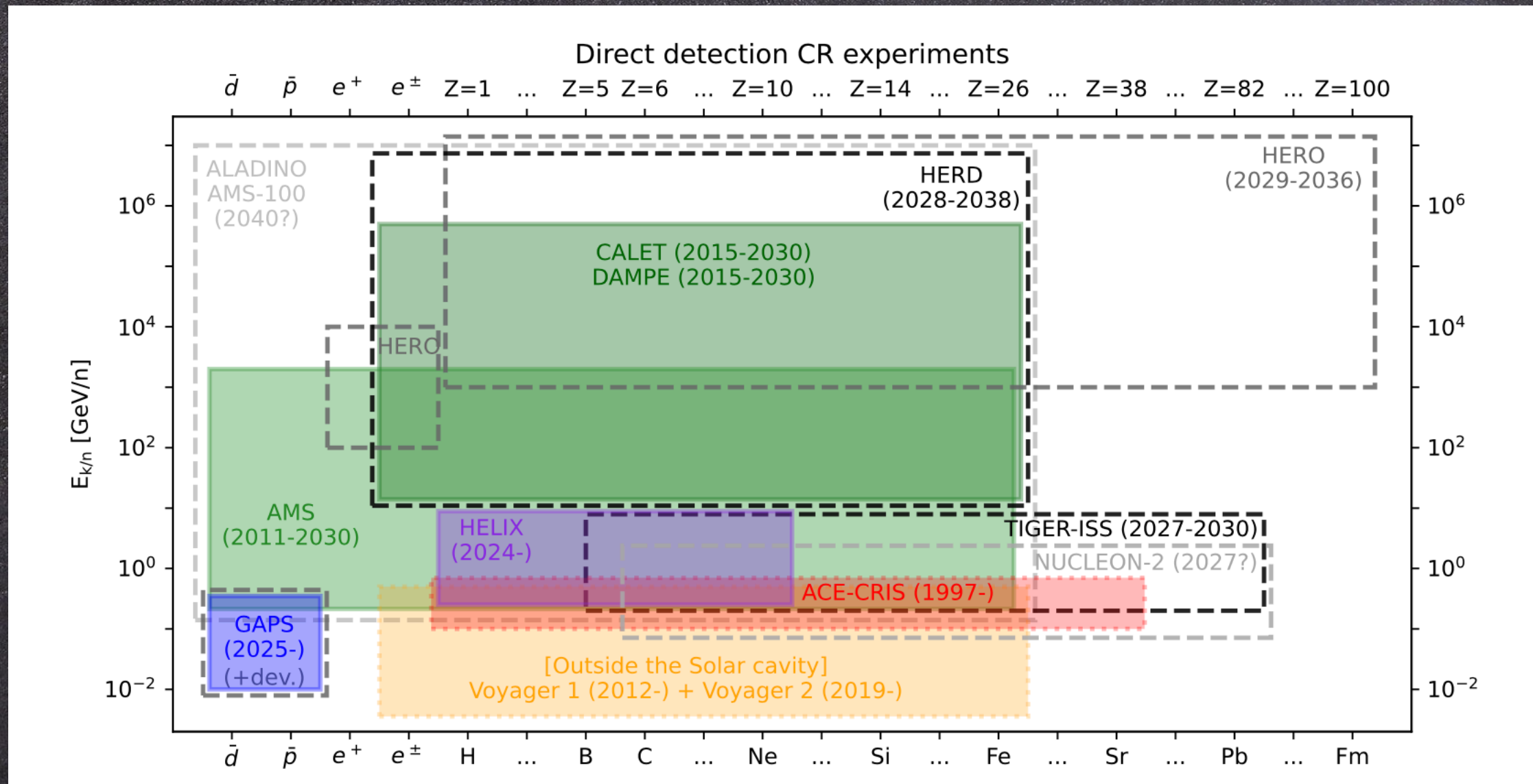
The Galaxy seen by a wandering particle

Geometry: can be approximated to a cylinder, with the thin galactic disc and a thick magnetic halo



Solution of the eq.: semi-analytic (Maurin+ 2001, Donato+ 2004, Maurin 2018 ...) as USINE code, or fully numerical: GALPROP (Strong&Moskalenko 1998), DRAGON (Evoli+ 2008; 2016), PICARD (Kisskammann, 2014, Kisskammann+ 2015), ...

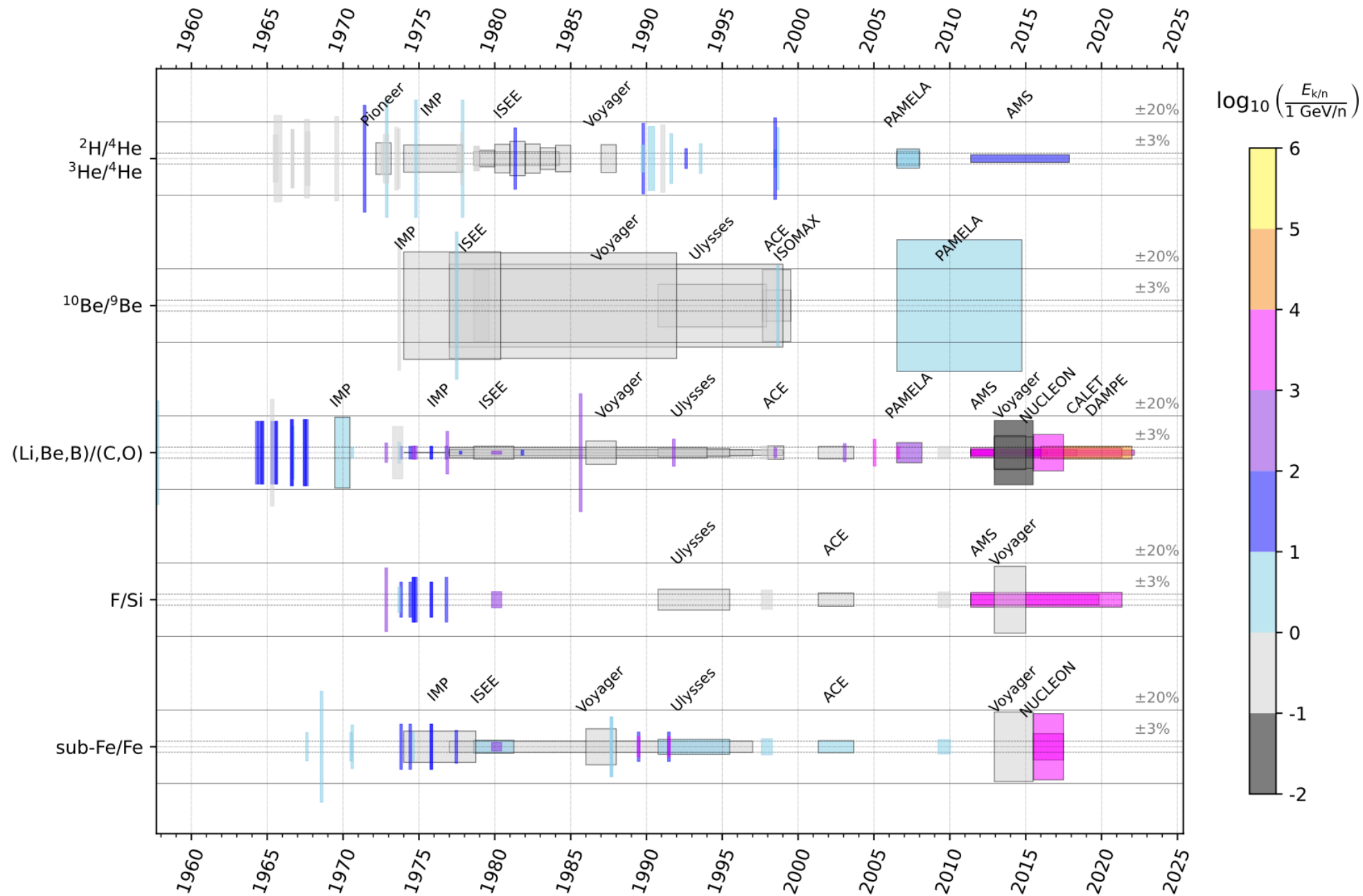
Cosmic ray experiments: species and energies



Voyager and ACE have outlasted their initial programme
AMS, CALET and DAMPE are running

Timeline of the highest energy decade and precision data on CRs

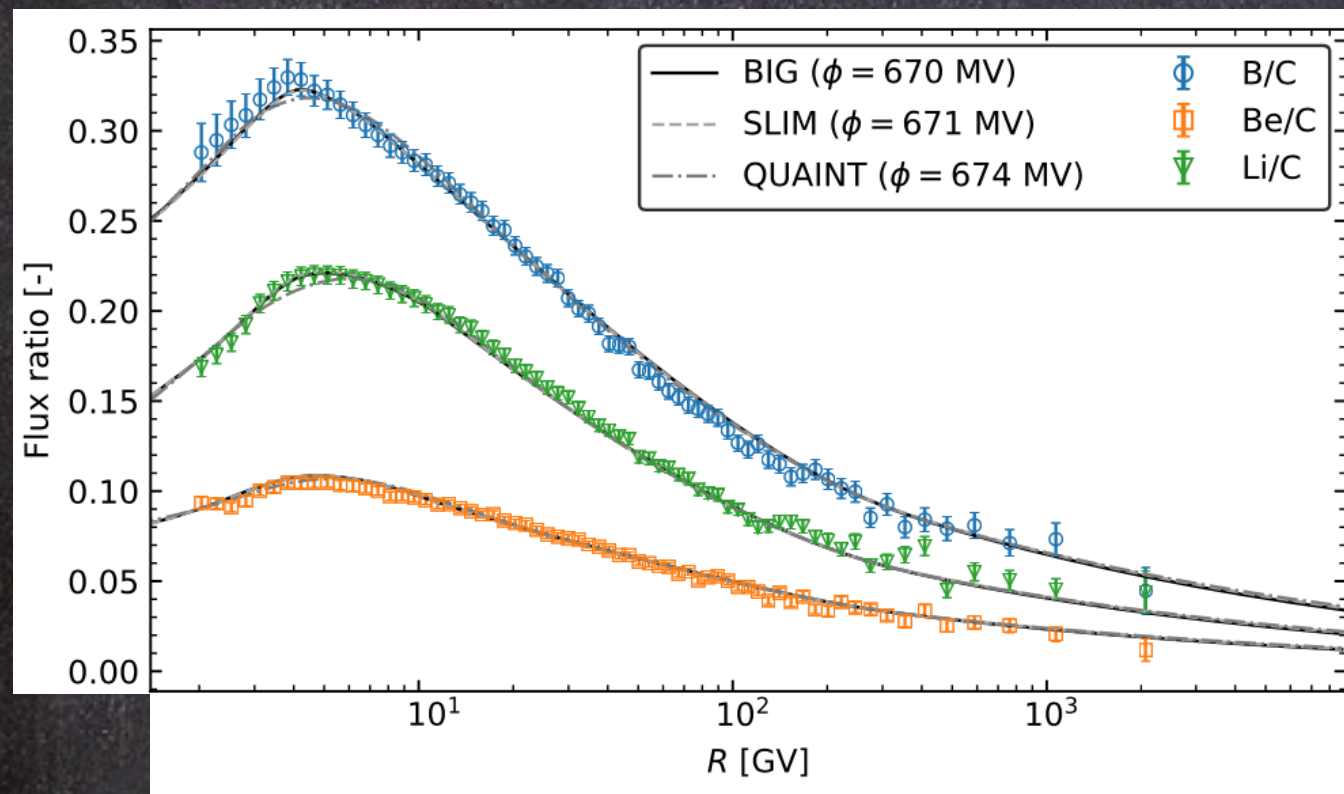
D. Maurin, FD et al., 2503.16173



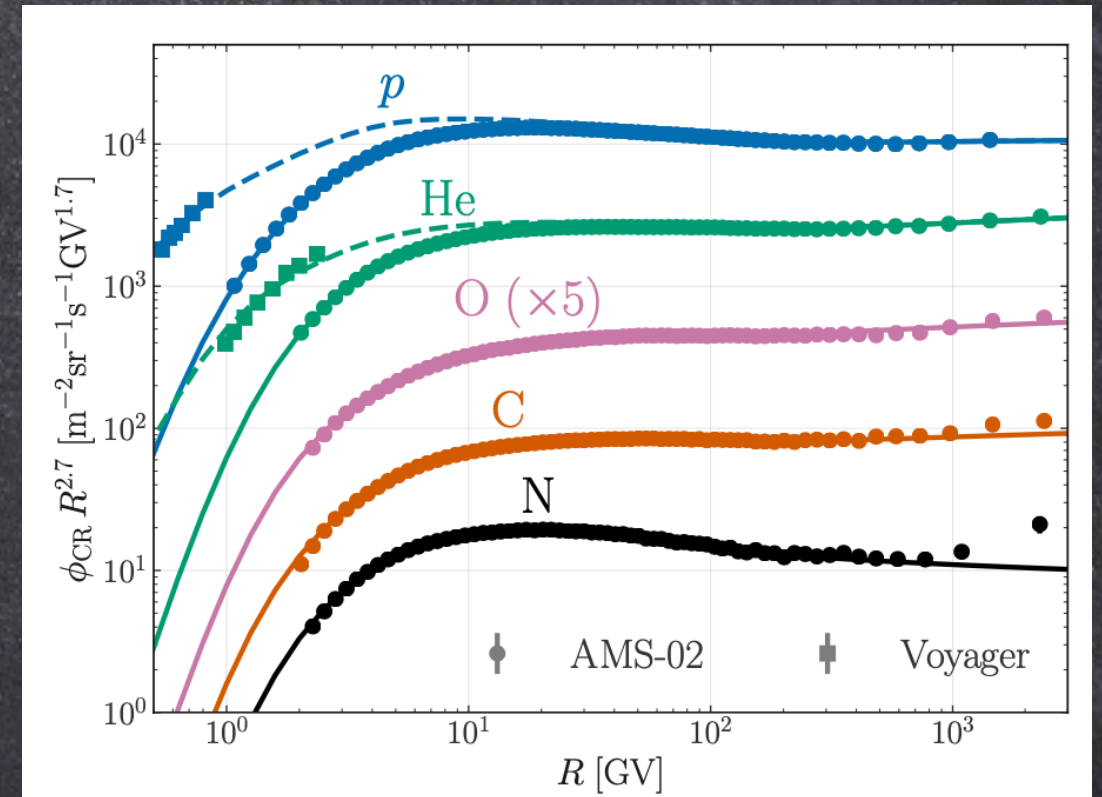
CR physics in space is precision physics

Propagation models vs data

Weinrich+ A&A 2020



Di Mauro, FD+ 2023



See also Evoli+ PRD 2020; Schroer+ PRD 2021; Cuoco&Korsmeier PRD 2021, 2022

Data on nuclear species are well described by propagation models with diffusion coefficient ($D \propto R^{\delta}$) power index $\delta = 0.50 \pm 0.03$

Convection or reacceleration models both work

Interpretations (all!) hampered by cross sections

Cross sections for Galactic CRs: a step forward

<https://indico.cern.ch/event/1377509/> @ CERN, 10/2024
(D. Maurin, FD, S. Mariani)

Precision cross-sections for advancing cosmic-ray physics and other applications: a comprehensive programme for the next decade

D. Maurin^{a,*}, L. Audouin^b, E. Berti^c, P. Coppin^d, M. Di Mauro^e, P. von Doetinchem^f,
F. Donato^{e,g,h}, C. Evoli^{i,j}, Y. Génolini^k, P. Ghosh^l, I. Leya^m, M. J. Losekamm^{n,o}, S. Mariani^h,
J. W. Norbury^p, L. Orusa^{q,r}, M. Panizza^d, T. Poeschl^h, P. D. Serpico^k, A. Tykhonov^d,
M. Unger^s, M. Vanstalle^t, M.-J. Zhao^{u,v}, D. Boncioli^{w,j}, M. Chiosso^{e,g}, D. Giordano^e,
D. M. Gomez Coral^x, G. Graziani^c, C. Lucarelli^h, P. Maestro^{y,z}, M. Mahleinⁿ, L. Morejon^{aa},
J. Ocampo-Peleteiro^{ab}, A. Oliva^{ab}, T. Pierog^t, L. Šerkšnytė^h

D. Maurin et al. 2503.16173, subm. to Physics Report

The role of cross sections in CR physics

D. Maurin, FD et al., 2503.16173

$$\frac{\partial \psi^j}{\partial t} - \nabla \cdot (\overline{\overline{D}} \nabla \psi^j) + \vec{u} \cdot \nabla \psi^j - \frac{1}{3} \nabla \cdot \vec{u} \left(p \frac{\partial \psi^j}{\partial p} \right) - \frac{1}{p^2} \frac{\partial}{\partial p} \left(p^2 D_{pp} \frac{\partial \psi^j}{\partial p} \right) =$$

$$q^j + \frac{1}{p^2} \frac{\partial}{\partial p} \left[p^2 \left(\frac{dp}{dt} \right) \psi^j \right] - \Gamma_{\text{tot}}^j \psi^j + \sum_i \psi^i \otimes \Gamma^{i \rightarrow j}.$$

$$\Gamma_{\text{tot}}^j = \frac{1}{\gamma \tau_{\text{dec}}^j} + \sum_t n_{\text{ISM}}^t v \sigma_{\text{inel}}^{j+t}$$

Destruction by decay or inelastic scattering

$$\psi^i \otimes \Gamma^{i \rightarrow j} = \sum_t n_{\text{ISM}}^t \int dE_{\text{k}}^i v \frac{d\sigma_{\text{prod}}^{i+t \rightarrow j}}{dE_{\text{k}}^j} (E_{\text{k}}^i, E_{\text{k}}^j) \psi^i(E_{\text{k}}^i)$$

Production from spallation
(secondary species)

Typically: the beam is the incident CR flux,
the target is the interstellar medium (90% H, 10% He)

Definitions for cross sections

$$\sigma_{\text{tot}} = \sigma_{\text{el}} + (\sigma_{\text{quasi-el}} + \sigma_{\text{prod}}) = \sigma_{\text{el}} + \sigma_{\text{inel}}$$

$$\sigma_{\text{inel}} = \sigma_{\text{quasi-el}} + \sigma_{\text{prod}}$$

If projectile i and target j :

Total: $i + j \rightarrow X$

Elastic: $i + j \rightarrow i + j$

Quasi-elastic: $i + j \rightarrow i + j + X$

Production: $i + j \rightarrow X$ not i

N.B. other notations: reaction for inelastic, absorption for production XS

Some notations about cross sections

$$\sigma_{\text{inv}} = E \frac{d^3\sigma}{dp^3} = \frac{E}{\pi} \frac{d^2\sigma}{dp_L dp_T^2}$$

- σ_{inv} Lorentz invariant cross section
- E total energy of the fragment
- p_L longitudinal momentum
- p_T transverse momentum
- $x_R = E^*/E_{\text{max}}^*$ radial scaling
- $x_F = 2p_L^*/\sqrt{s}$ Feynman scaling
- E^*, p_L^* in the centre-of-mass frame
- $\sqrt{s} = (m_i^2 + m_j^2 + 2E_i m_j)^{1/2}$
- m_i and E_i mass and total energy of the GCR projectile
 m_j the mass of the ISM target (at rest).

N.B.: in the Galaxy, we integrate on the angles

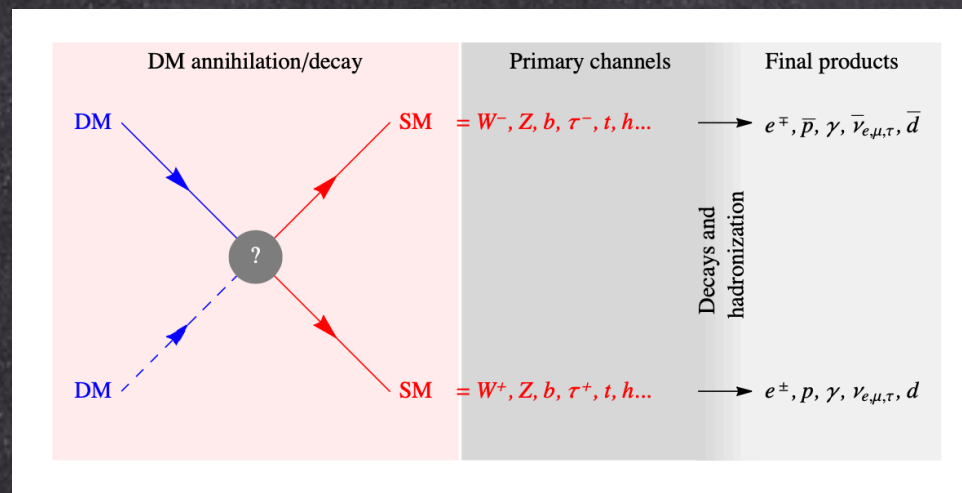
Physics cases with Xs

1. Can we reveal dark matter with CRs?
2. Where are GCRs synthesized and accelerated? How?
3. GCR transport
4. Hypothesis for Galactic sources
5. Transverse topics (cosmogenic studies, space exploration, hadrontherapy, ultra-high energy CRs, equation-of-state for neutron stars...)

Indirect Dark Matter detection in Cosmic Rays

Dark Matter (DM) Annihilation or decay:

γ -rays (diffuse, monochromatic line), X-rays and radio, neutrinos,
antimatter, searched as RARE COMPONENTS in cosmic rays (CRs):
antiprotons, positrons, antideuterons, antihelium



ν and γ keep directionality

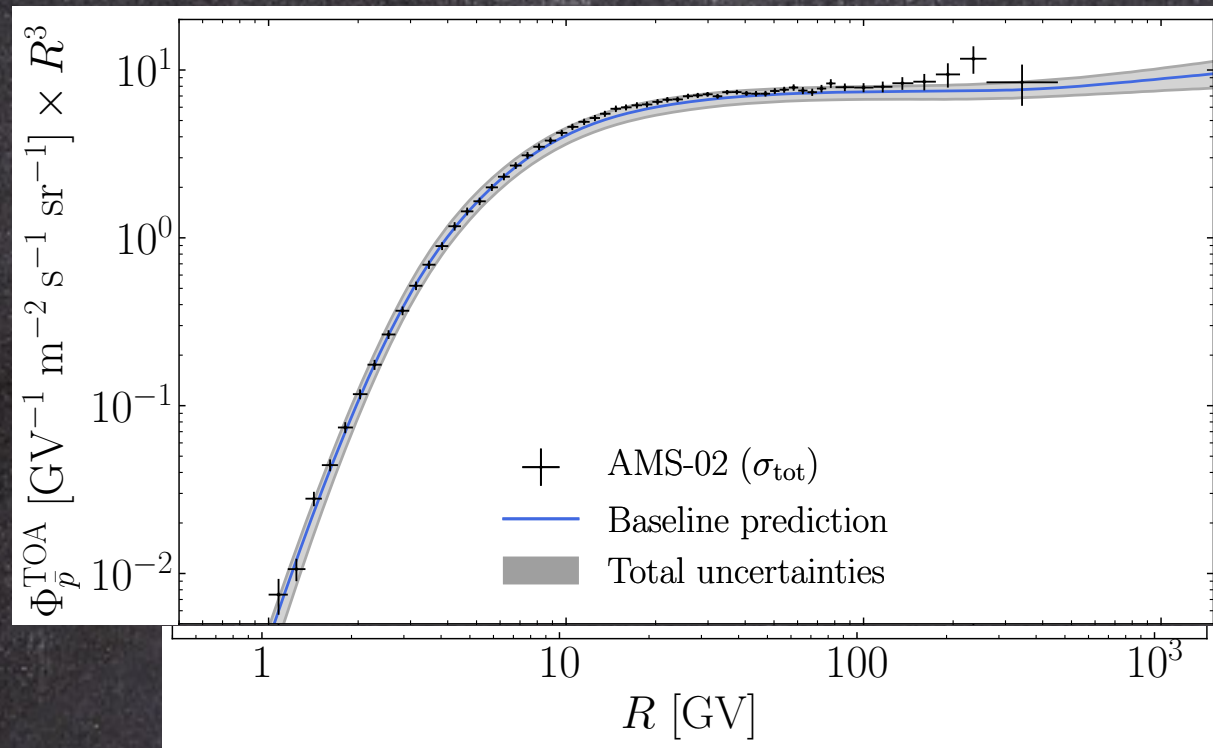
Charged particles diffuse in the galactic halo

ASTROPHYSICS OF COSMIC RAYS

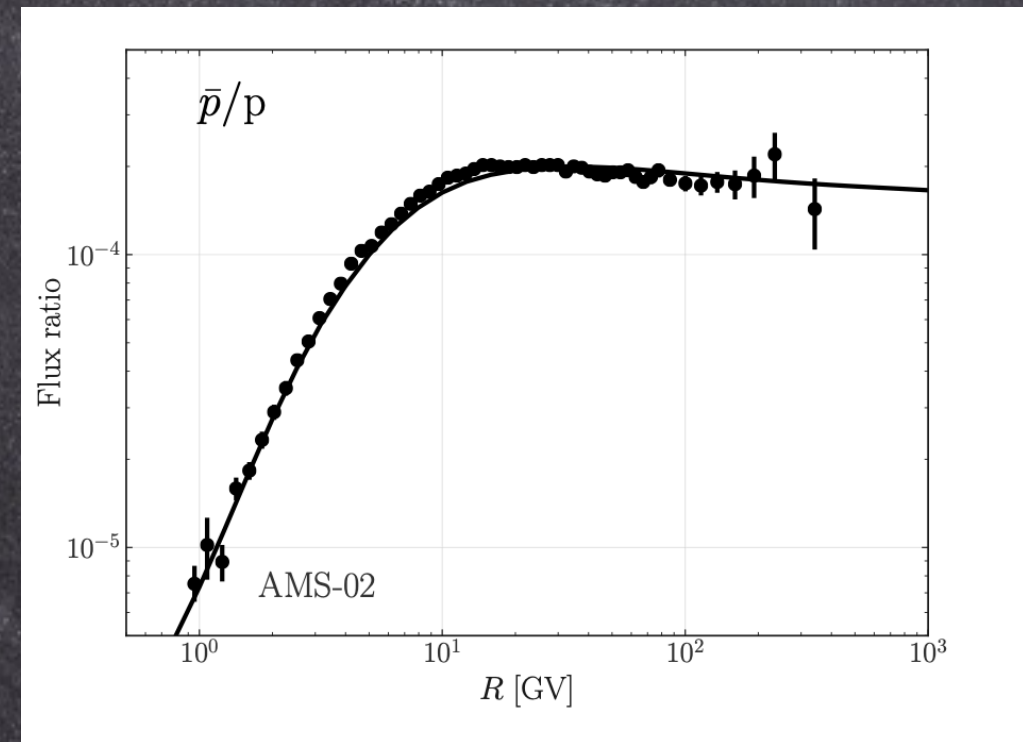
Secondary antiprotons in CRs

Secondary CRs: via spallations of CRs on the interstellar medium

M. Boudaud+ PRD 2020



Di Mauro, Korsmeier, Cuoco PRD 2024



- Secondary pbar flux is predicted consistent with AMS-02 data
- Transport and cross section uncertainties are comparable
- A tiny dark matter contribution cannot be excluded
- Precise predictions are mandatory

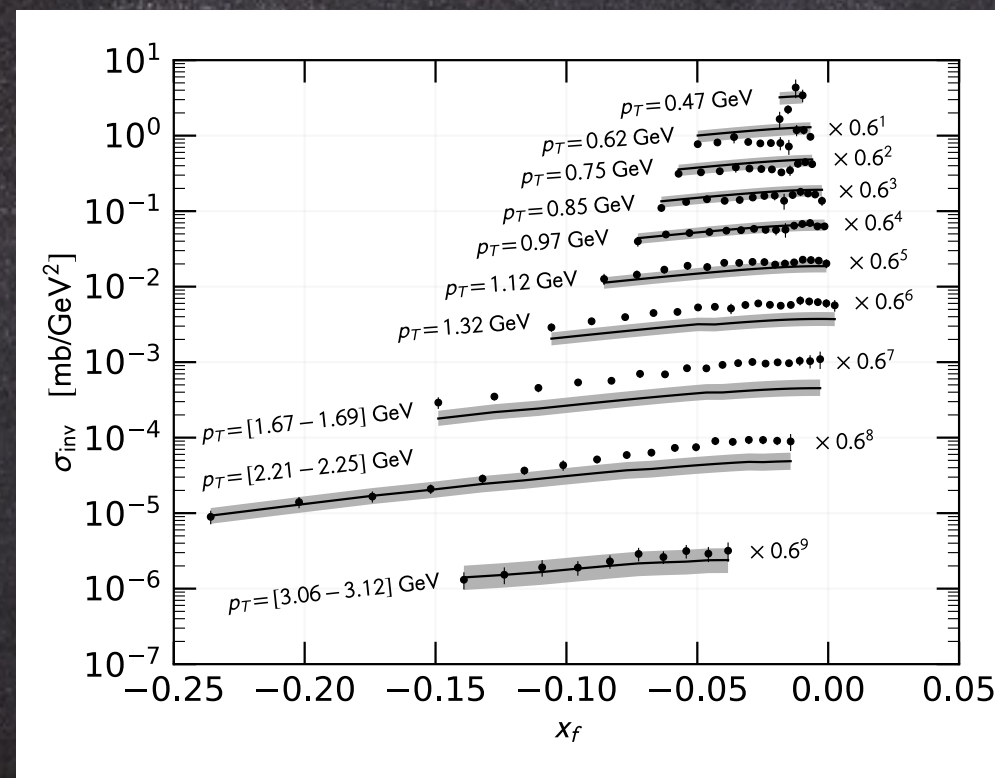
See also Feng, Tomassetti, Oliva 2016; Korsmeier, FD, Di Mauro PRD 2018, Reinert & Winkler JCAP2018;
De La Torre Luque+ JCAP2024

High-energy antiproton cross sections

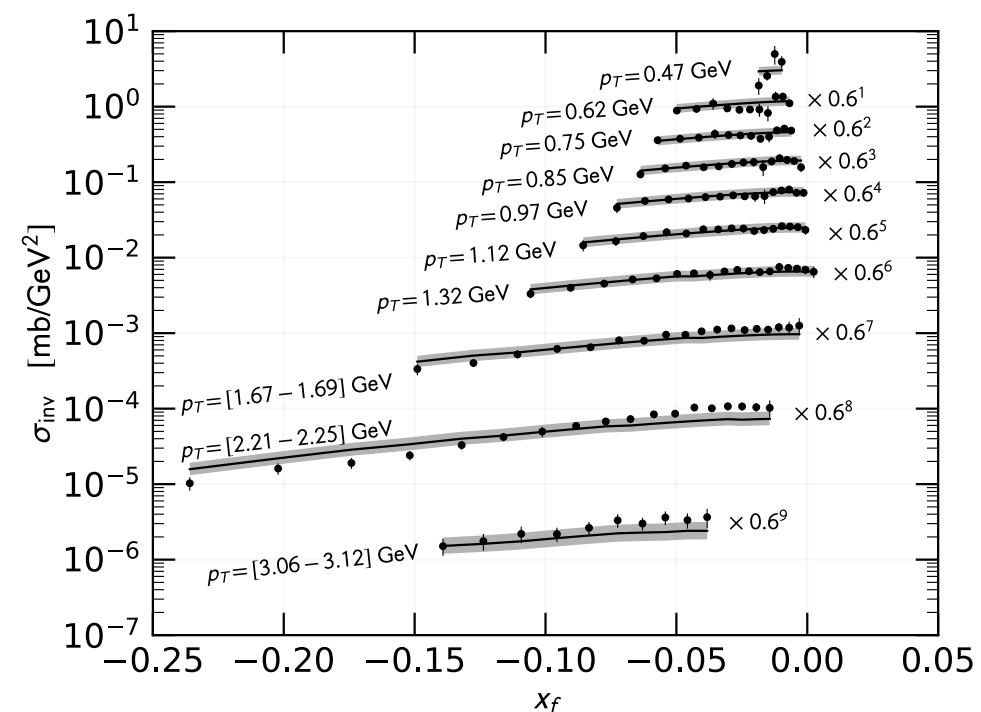
Korsmeier, FD, Di Mauro, PRD 2018
LHCb Coll. PRL2018

1. Fit to NA61 $pp \rightarrow p\bar{b} + X$ data
2. Calibration of pA XS on NA49 $pC \rightarrow p\bar{b} + X$ data
3. Inclusion of LHCb fixed target $pHe \rightarrow p\bar{b} + X$ data

Parametrization I



Parametrization II

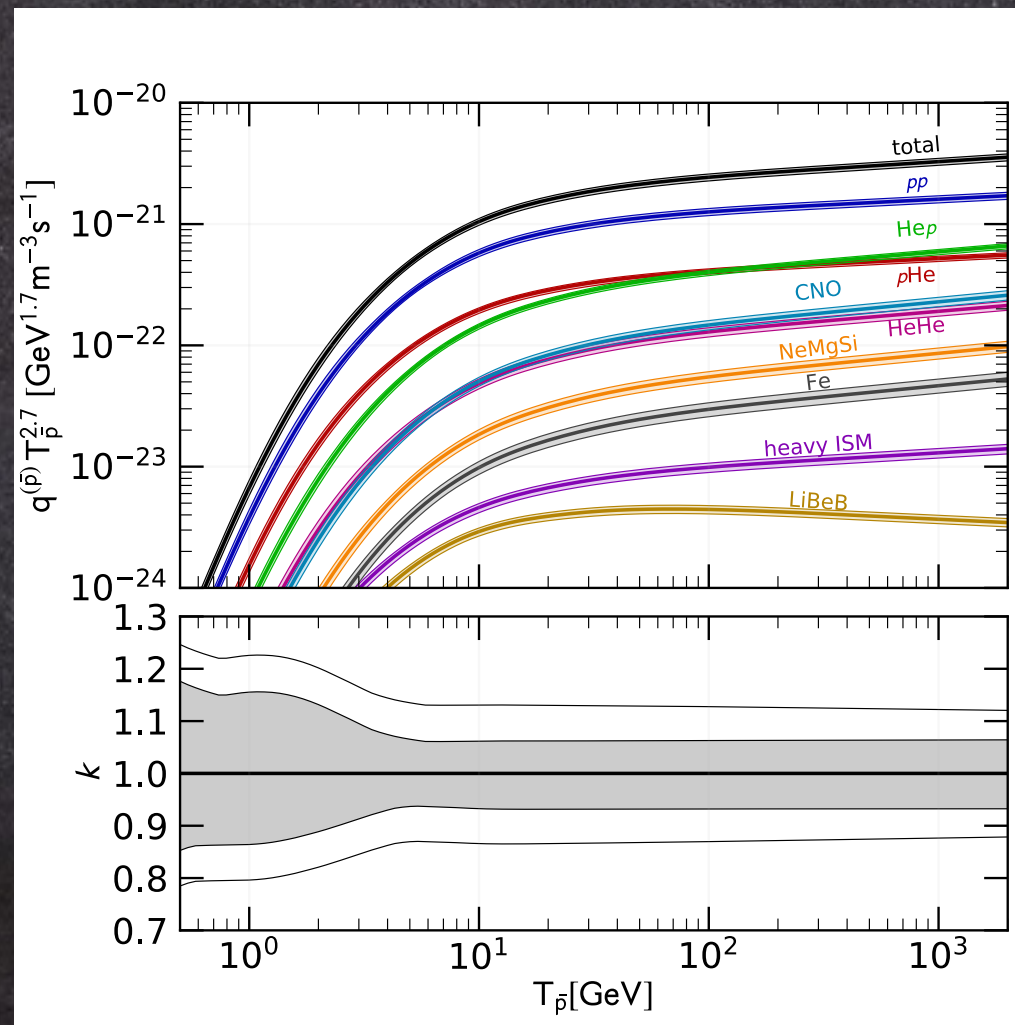


LHCb data agree better with pp Parameterizations II.
They select the high energy behavior of the Lorentz invariant cross section

Effects on the total pbar production

Korsmeier, FD, Di Mauro PRD 2018

$$q_{ij}(T_{\bar{p}}) = \int_{T_{\text{th}}}^{\infty} dT_i \, 4\pi n_{\text{ISM},j} \phi_i(T_i) \frac{d\sigma_{ij}}{dT_{\bar{p}}}(T_i, T_{\bar{p}}). \quad q_{ij}(T_{\bar{p}}) = \int_{T_{\text{th}}}^{\infty} dT_i \, 4\pi n_{\text{ISM},j} \phi_i(T_i) \frac{d\sigma_{ij}}{dT_{\bar{p}}}(T_i, T_{\bar{p}}).$$



Result with uncertainties
in the hyperon correction
and isospin violation

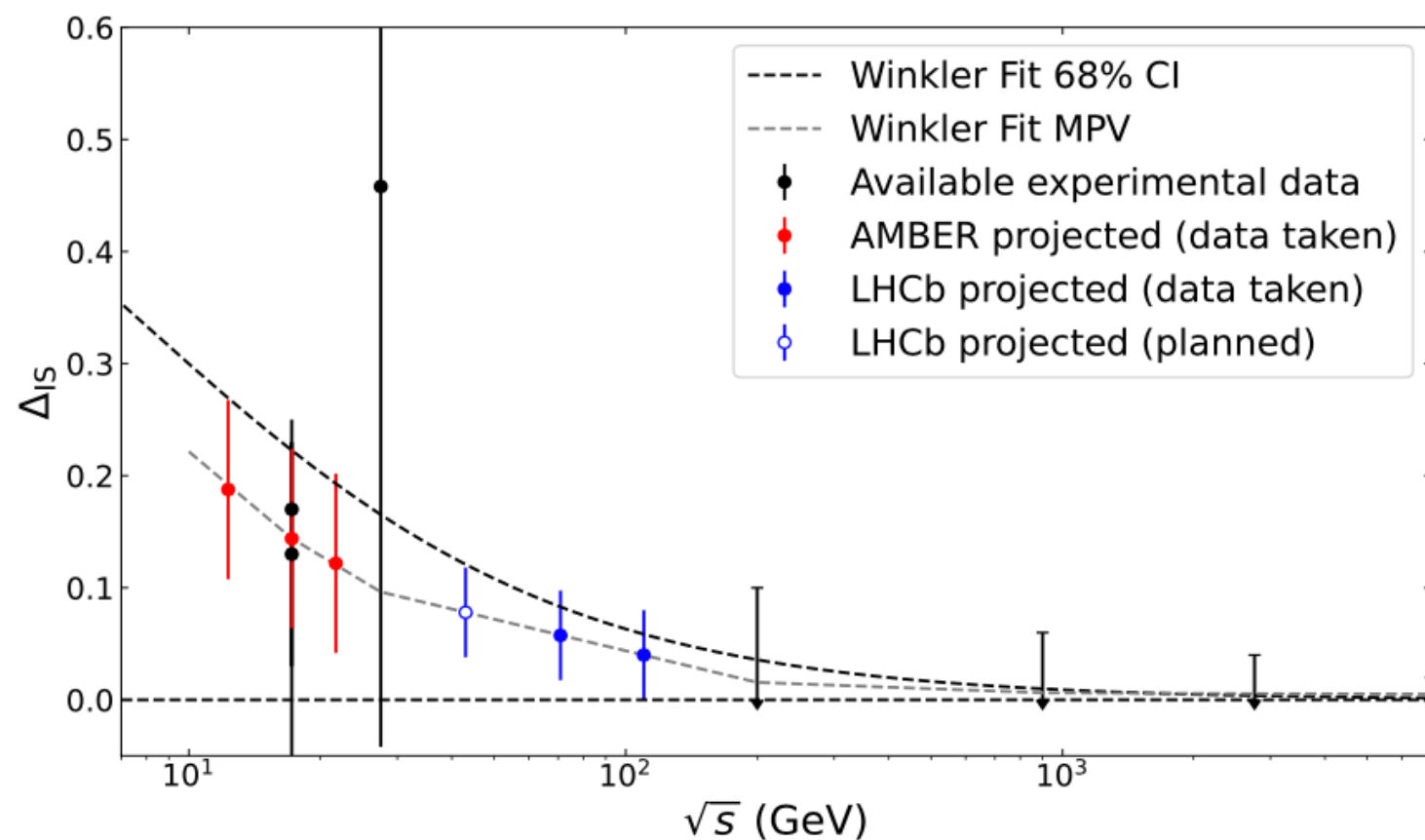
The antiproton source term
is affected by uncertainties of
 $\pm 10\%$ from cross sections.

Higher uncertainties
at very low energies

Isospin violation and enhancement?

$$\sigma_{\text{inv}}^{\text{Galaxy}} = \sigma_{\text{inv}}(2 + \Delta_{\text{IS}} + 2\Delta_{\Lambda})$$

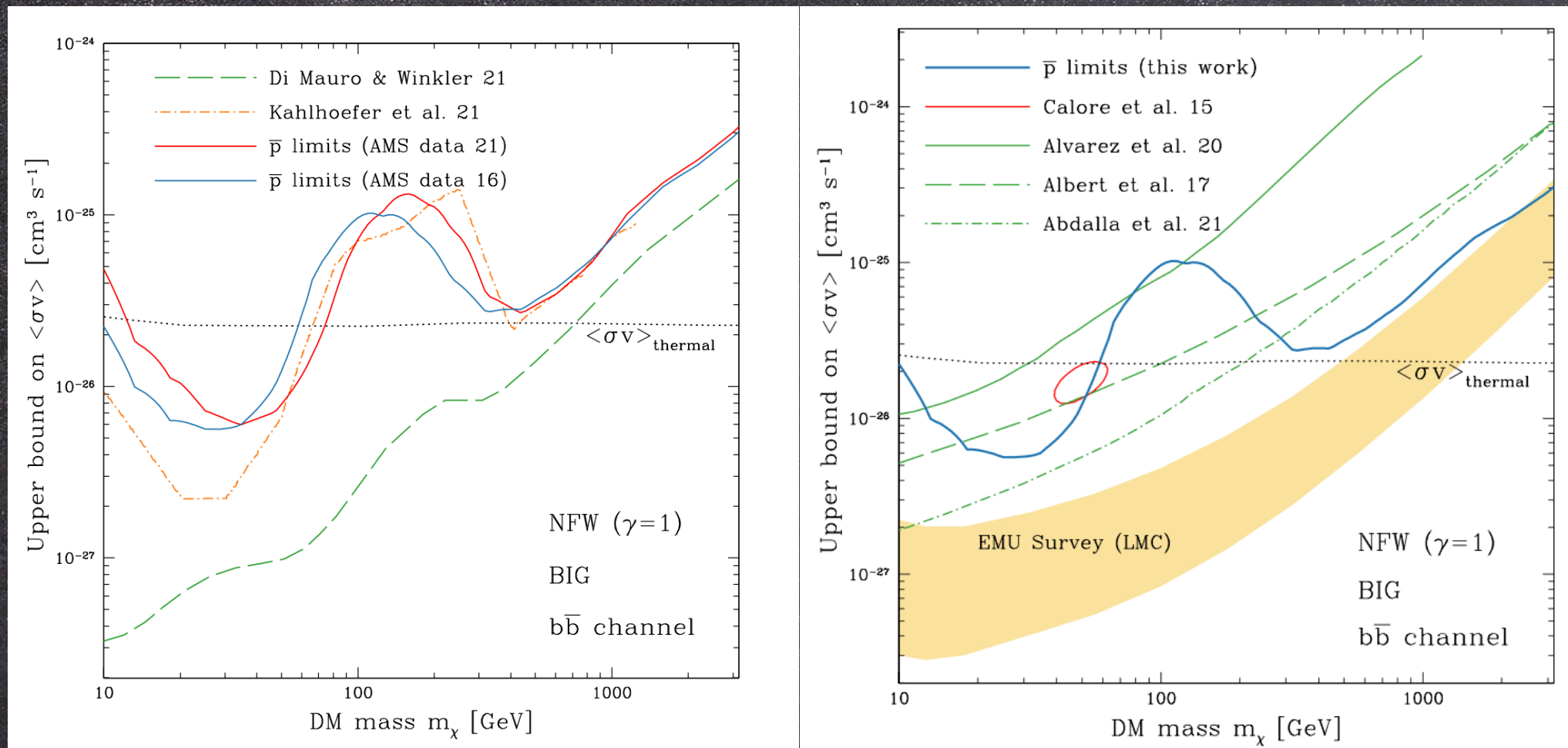
Traditionally, one multiplies by 2 for antineutron in pp scatterings.
In H.Fischer for NA49 (2003) an isospin asymmetry is claimed, with an enhancement in antineutron production.



Impact of Amber and LHCb measurements on the uncertainties of a potential isospin asymmetry production of antiprotons and antineutrons

Bounds on annihilating DM

Calore, Cirelli, Derome, Genolini, Maurin, Salati, Serpico, ScyPostPh 2022



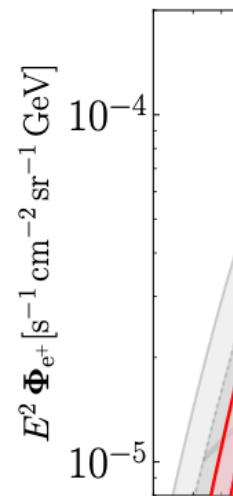
Err. data / model	local signif. [σ]	m^* [GeV]	$\langle\sigma v\rangle^*$ [cm^3/s]
cov/cov	1.81	109.3	1.71e-26
cov/none	2.39	10.5	5.07e-26
diag/cov	3.33	98.8	2.14e-26
diag/none	2.75	8.5	1.70e-25
stat/cov	5.19	89.7	1.48e-26
stat/none	4.49	8.0	2.98e-25

Correlation matrices for data and model are included.
They strongly influence a hint for DM

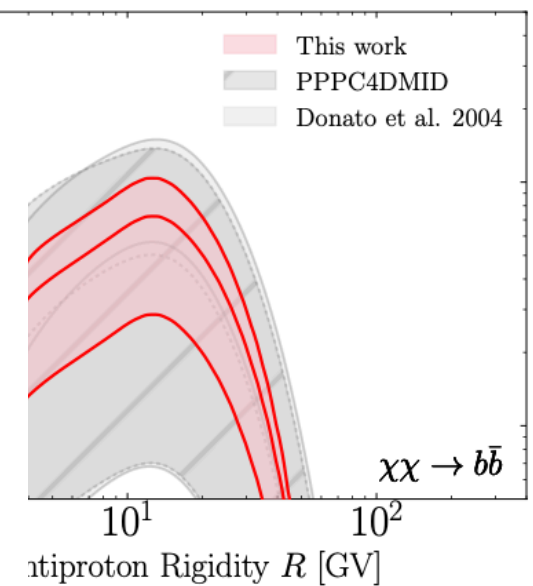
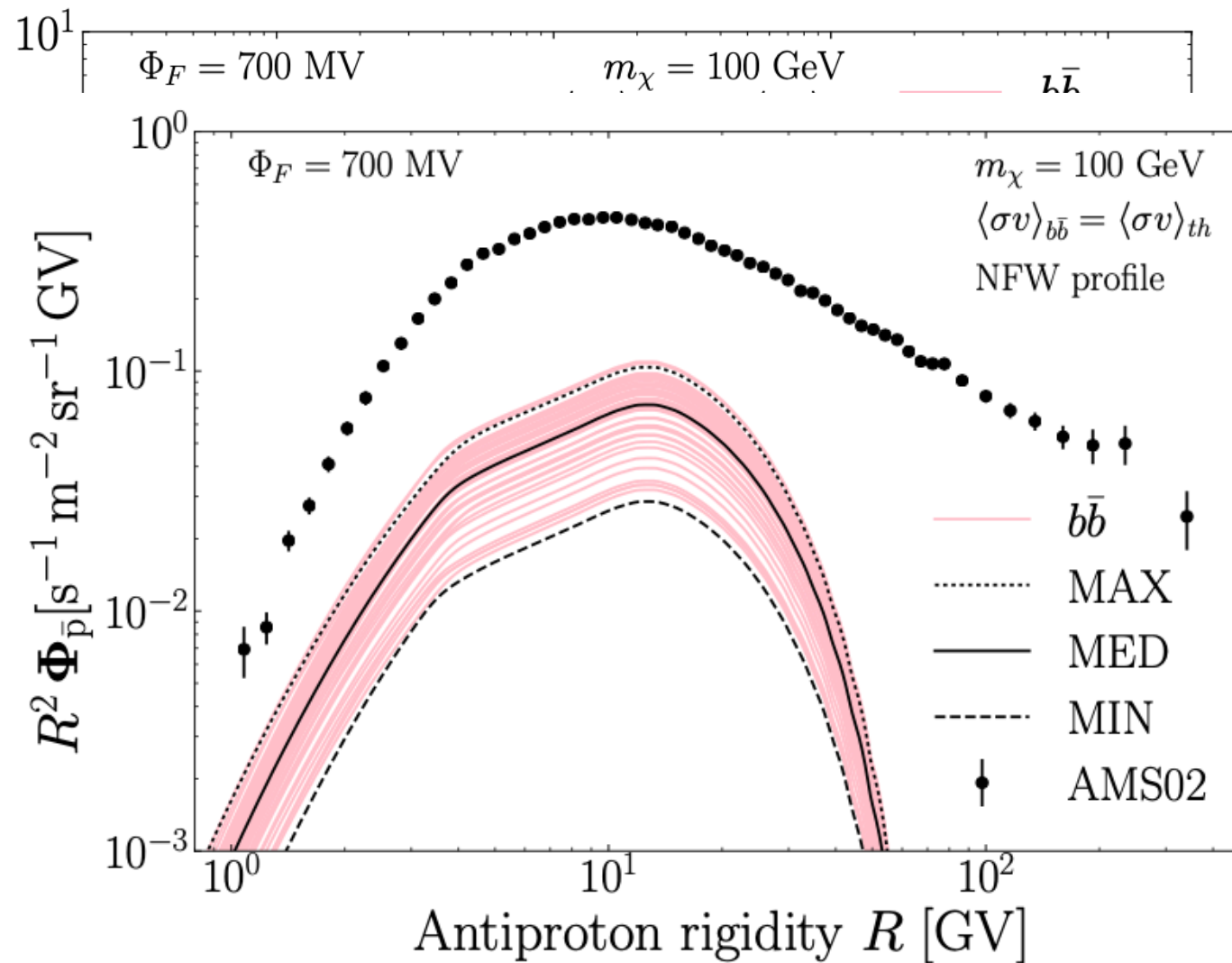
Effect of galactic propagation

Genolini+ PRD2021

New AMS-02 sec/prim data allow reduction of propagation uncertainties



$E^2 \Phi_{e^+} [\text{s}^{-1} \text{m}^{-2} \text{sr}^{-1} \text{GeV}]$



Small effects by inhomogeneous diffusion Tovar-Pardo+ JCAP 2024

Antideuteron from relic WIMPS

FD, Fornengo, Salati PRD 62 (2000)043003

Baer & Profumo 2005; FD, Fornengo, Maurin PRD 2008; Fornengo+ 2013; Ibarra & Wild 2013; Hermis+ 2017

In order for fusion to take place, the two antinucleons must have low kinetic energy

Kinematics of spallation reactions prevents the formation of very low energy antiprotons (antineutrons).

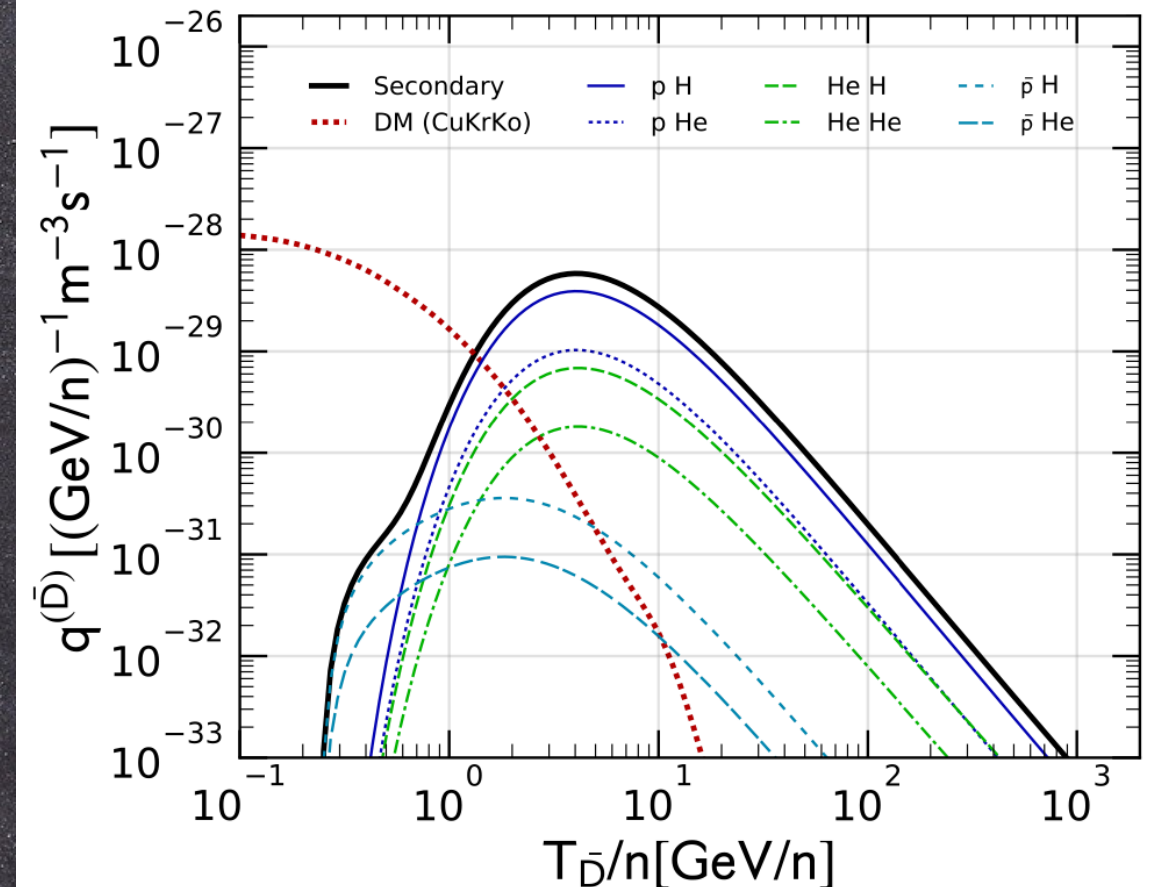
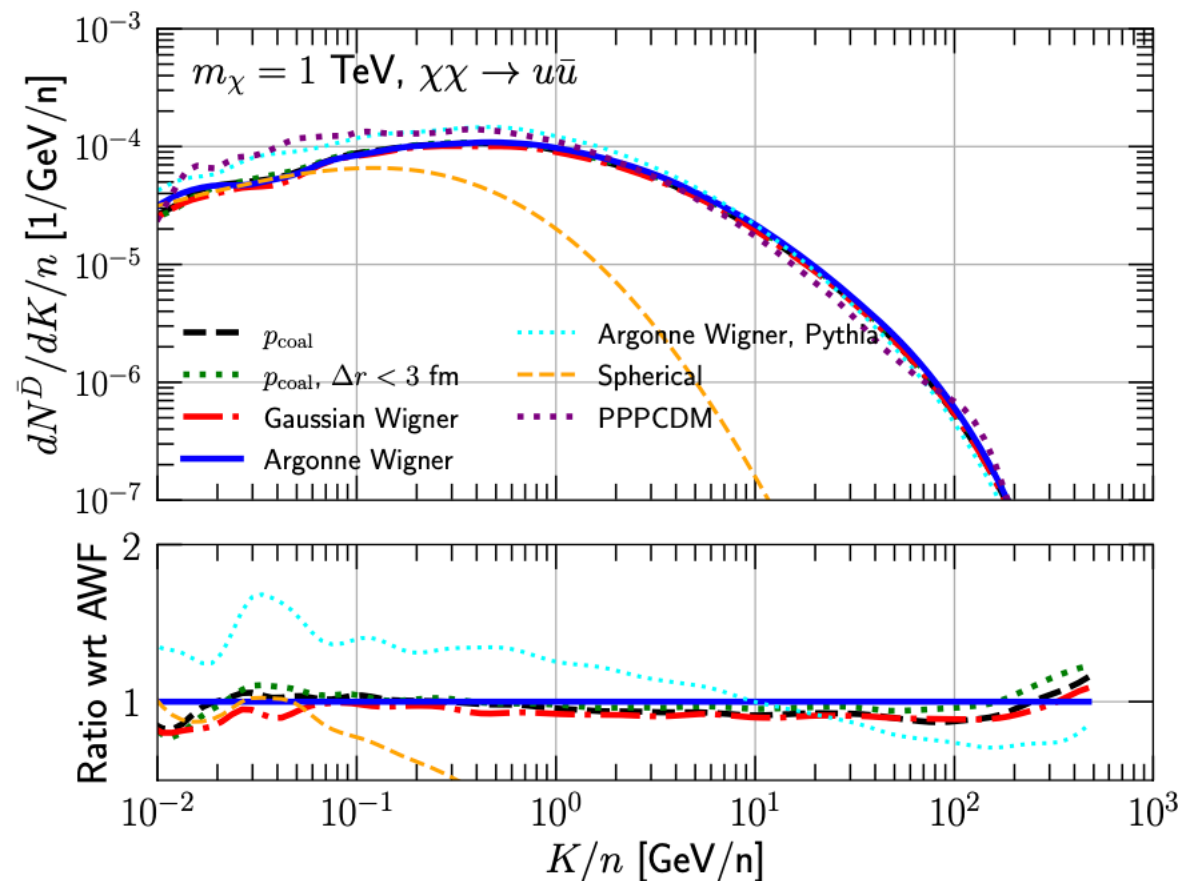
At variance, dark matter annihilates almost at rest

Secondary and DM have different kinematics and source spectra.
Below few GeV/c solar modulation spread spectra similarly

Fusion process and source spectra

Di Mauro+2411.04815

Korsmeter, FD, Fornengo PRD 2018



Coalescence treated according to Wigner Formalism does not add significant uncertainties

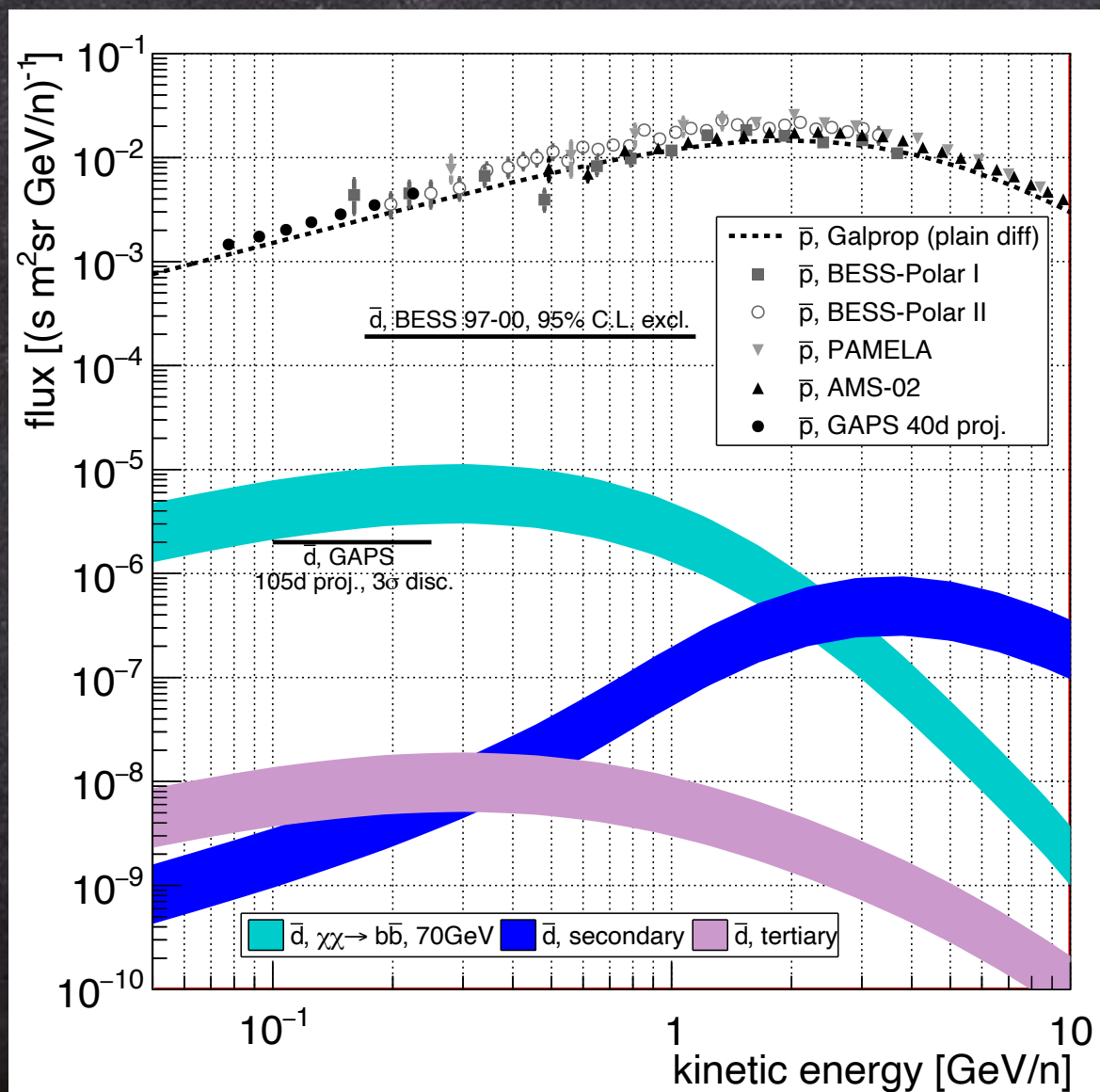
Window DM/secondary below 1 GeV/n

Kachelriess, Ostapchenko, Tiemsland EurPhysJA 2020

Antideuteron in cosmic rays

FD, Fornengo, Salati PRD 62 (2000)043003 P. Von Doetinchem et al. Phys. Rep. 2021

GAPS experiment will operate in Antarctica



AMS-02 antiproton data

Antideuteron predictions
for DM model indicated by
pbar AMS-02 data

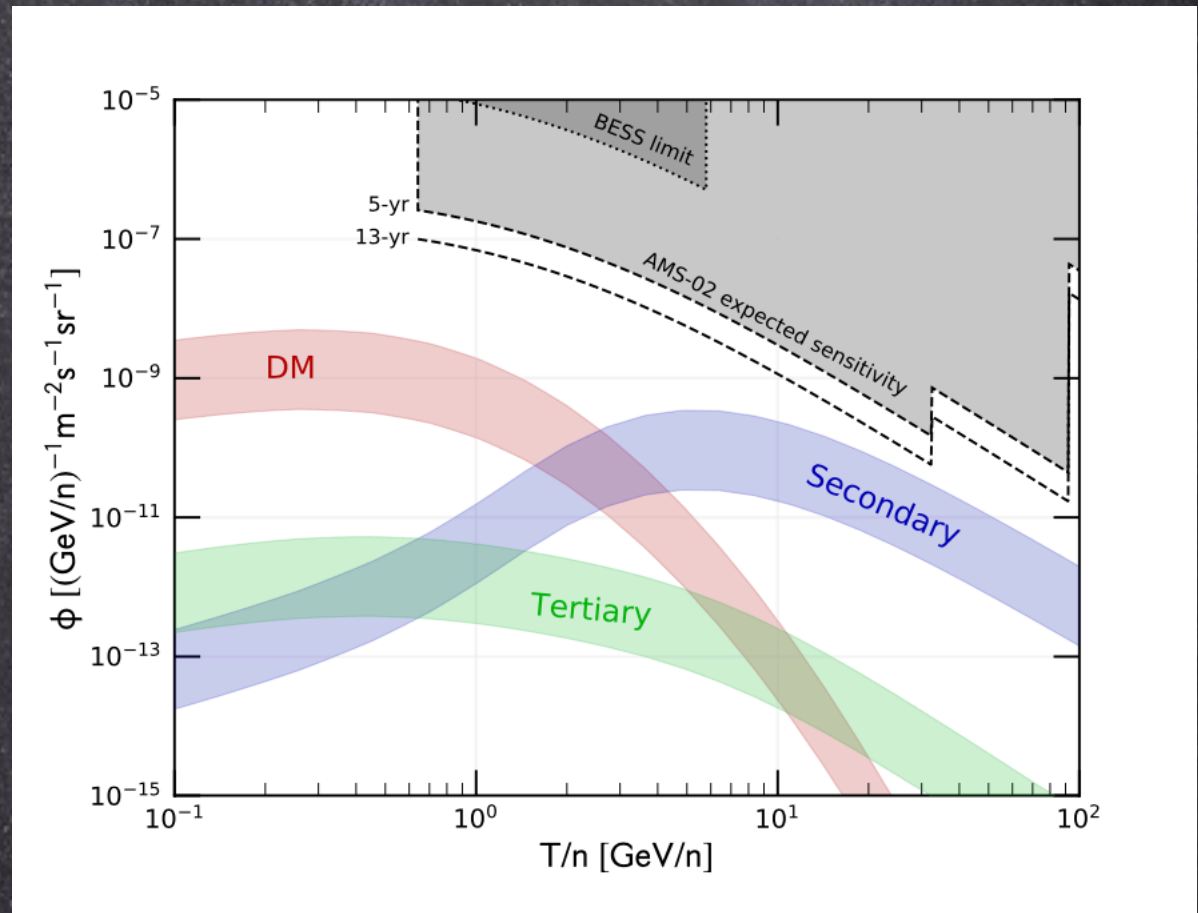
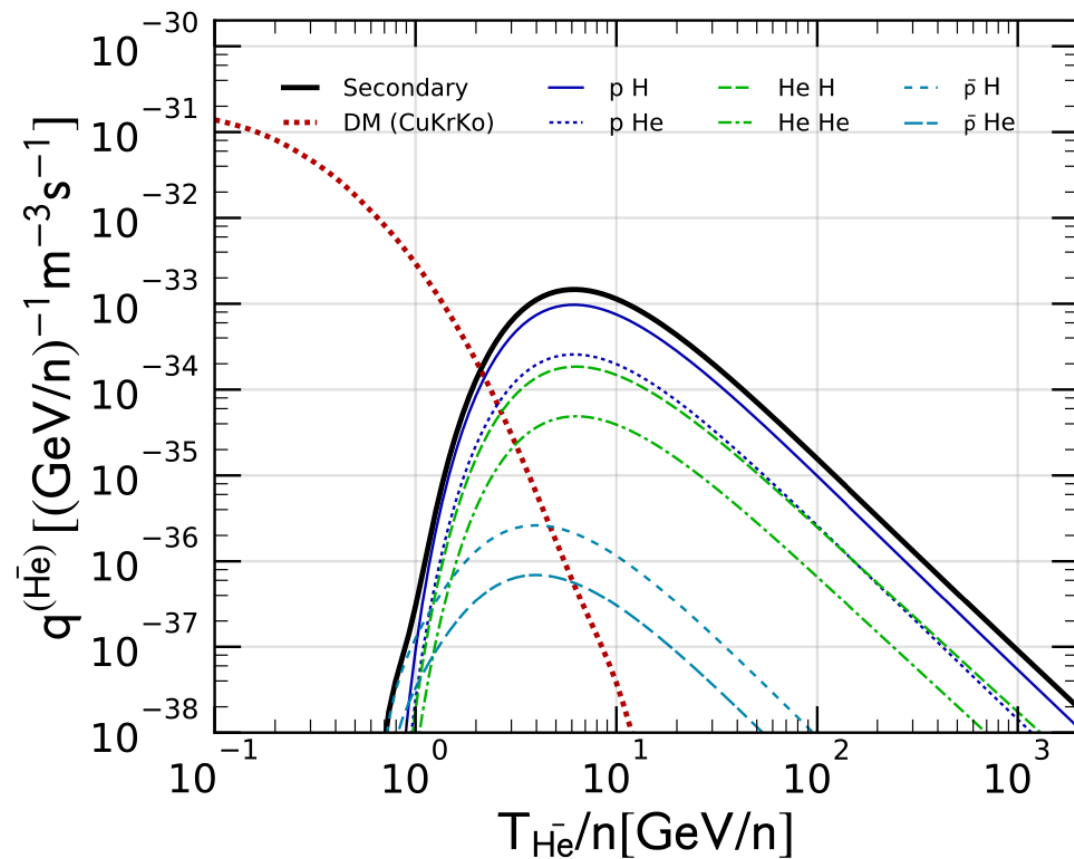
Bands are for coalescence
uncertainty

Donato+ PRD 2008; Ibarra&Wild PRD, JCAP 2013; Fornengo+ JCAP 2013;
Tomassetti&Oliva ApJL2017; Aramaki+ Phys. Rep. 2021

Perspectives with antihelium

Cirelli+JHEP2014; Carlson+ PRD2014

FD, Fornengo, Korsmeier, PRD 2018



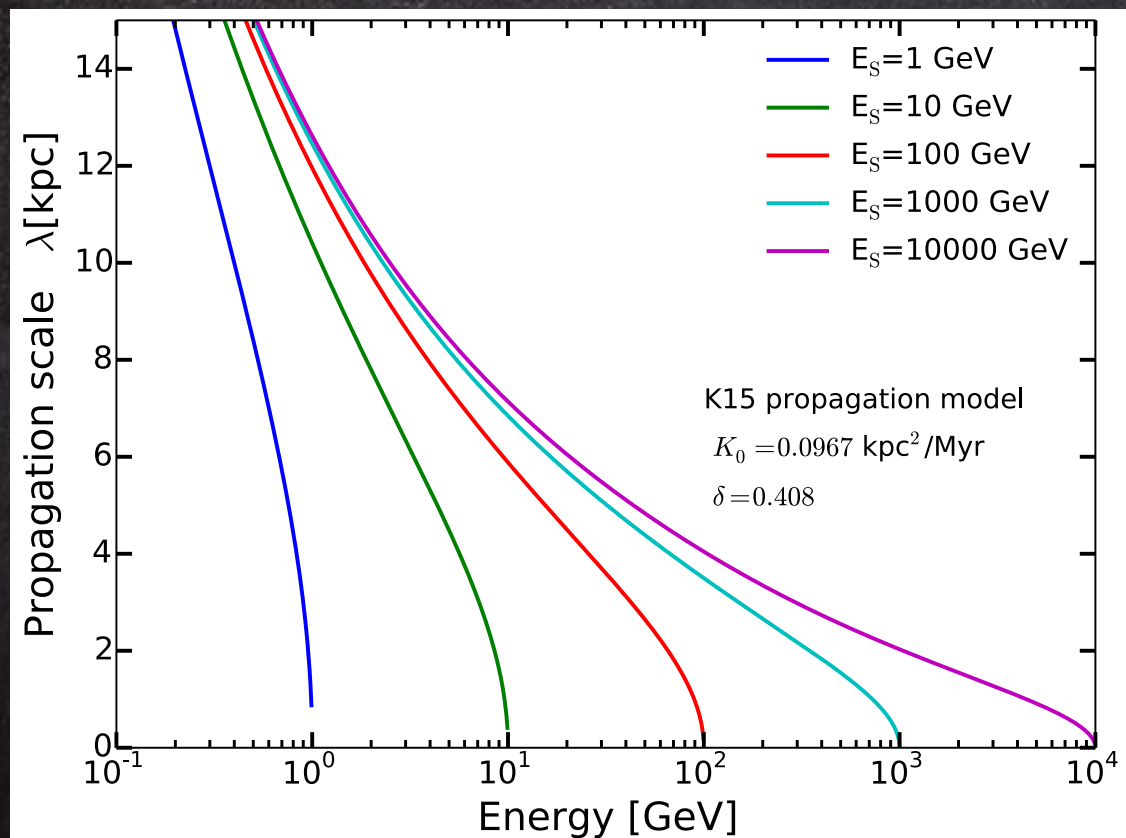
Very favorable DM/secondary window.
However, the flux is expected to be extremely low

Positrons and electrons are local probes

Typical propagation length in the Galaxy

$$\lambda^2(E, E_S) = 4 \int_E^{E_S} dE' \frac{D(E')}{b_{\text{loss}}(E')}$$

Manconi, Di Mauro, FD JCAP 2017



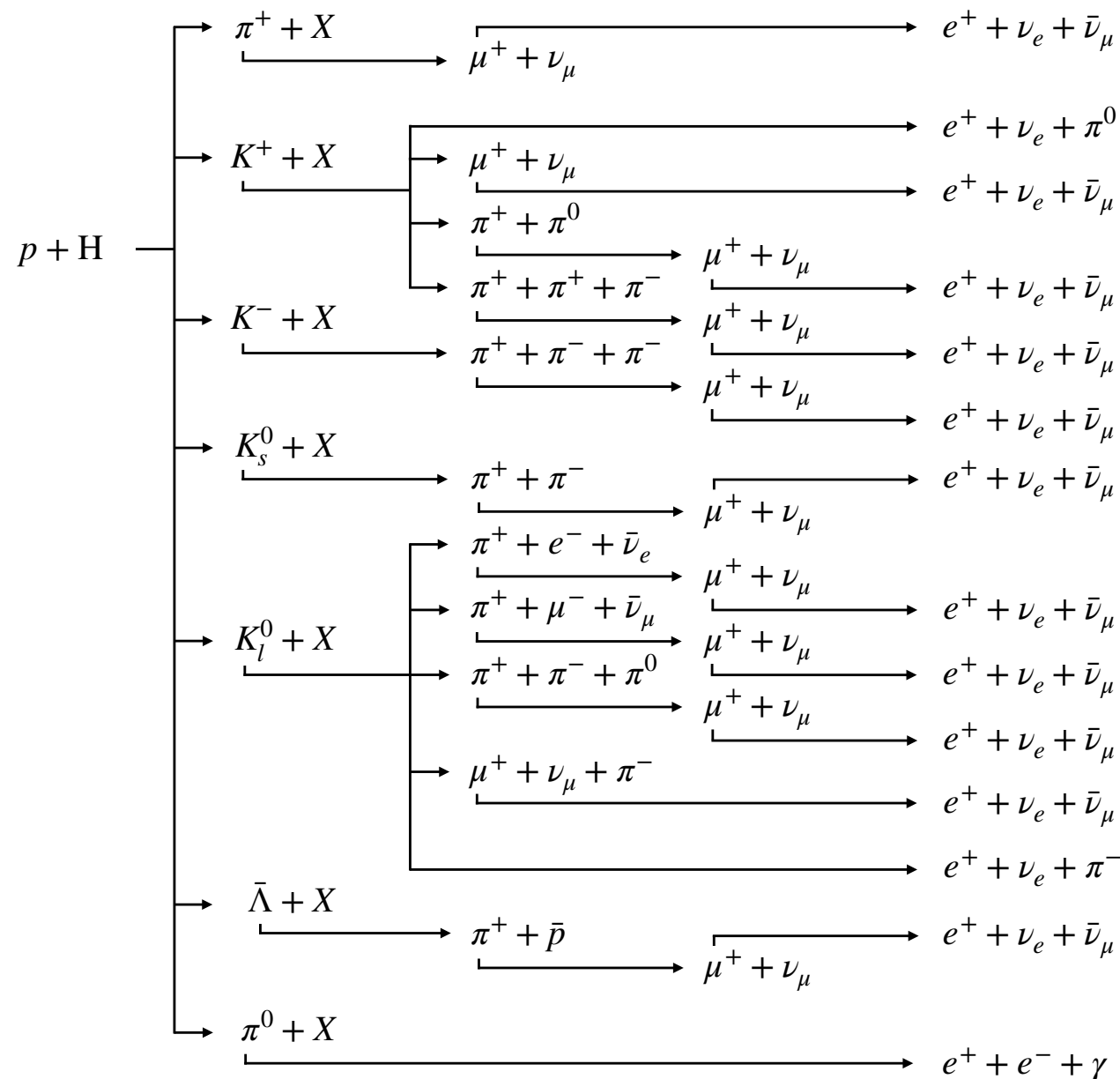
e^- , e^+ suffer strong radiative cooling by inverse Compton scattering and synchrotron radiation.

They arrive at Earth from few kpc:
Probe the very local Galaxy

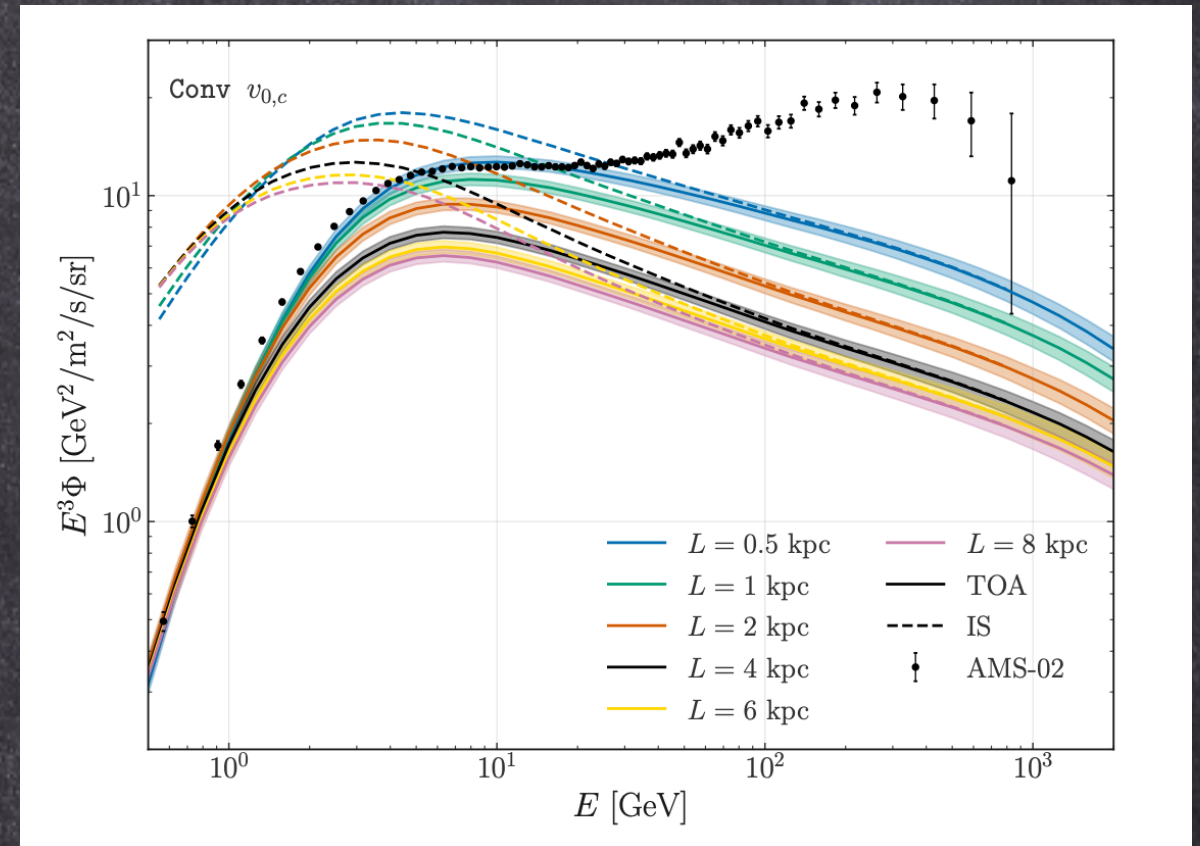
Secondary e^+ production channels

$$q_{ij}(T_{e^+}) = 4\pi n_{\text{ISM},j} \int dT_i \phi_i(T_i) \frac{d\sigma_{ij}}{dT_{e^+}}(T_i, T_{e^+})$$

L. Orusa, M. Di Mauro, FD, M. Korsmeier PRD 2022



Di Mauro, FD, Korsmeier, Manconi, Orusa, PRD 2023

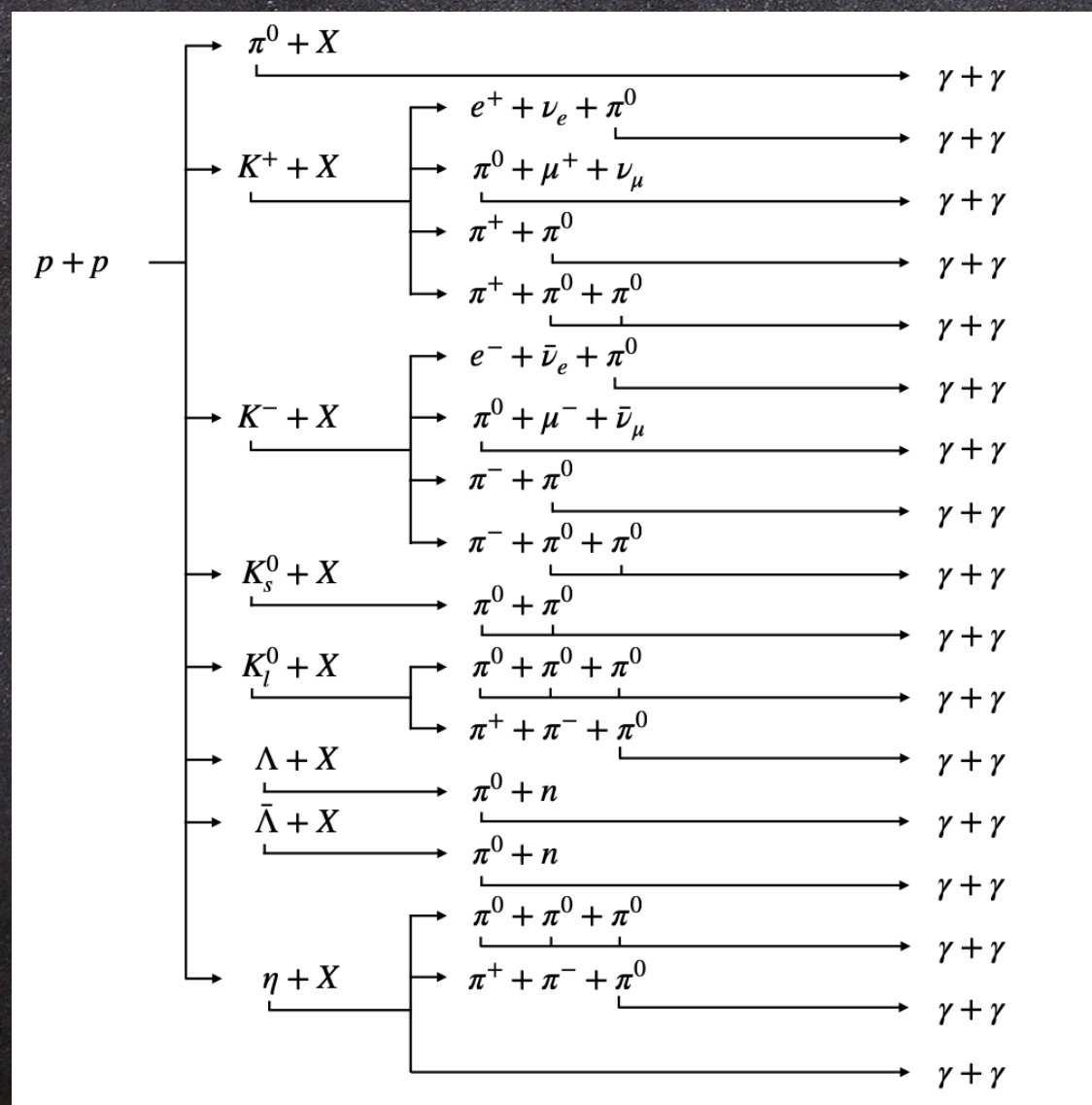


e^+ secondaries contribute significantly below few GeV
 Cross section uncertainties comparable to propagation ones at fixed halo size,
 5-7% in AMS-02 range

XS for γ -ray background (Fermi-LAT, CTA)

Orusa, Di Mauro, FD, Korsmeier PRD 2023

The main source of Galactic γ rays is from nucleon-nucleon interactions



Data on π^0 not available (or not usable),
a part LHCf

We relied on π^\pm

Uncertainties on production XS:
10% for $E_\gamma < 10\text{GeV}$, 20% above

Would need inclusive XS for
 $pp, pHe \rightarrow \gamma + X$

Accelerator data priorities for DM related searches

Spallation products are a background
to any search for new physics in CRs

D. Maurin, FD et al., 2503.16173

Table 3: Summary of the wish list of production cross-sections for GCRs that can be indirect probes of particle DM. Here, n_{tot} is the integrated multiplicity. The most pressing need is for \bar{p} , whose interpretation is already limited by cross-section uncertainties, but forthcoming CR data for \bar{d} , and possible $\overline{\text{He}}$ events from AMS, call for new cross-section measurements for these species. See text for the detailed motivations.

Particle	Reaction	Measurement	\sqrt{s}	Sought precision
\bar{p}	$p + p \rightarrow \bar{p} + X$	σ_{inv}	5 to 100 GeV	$< 3\%$
	$p + \text{He} \rightarrow \bar{p} + X$			$< 5\%$
	$p + p \rightarrow \bar{\Lambda} + X$			$< 10\%$
	$p + \text{He} \rightarrow \bar{\Lambda} + X$			$< 10\%$
	$p + p \rightarrow \bar{n} + X$			$< 5\%$
	$p + n \rightarrow \bar{p} + X$			$< 5\%$
\bar{d}	$p + p \rightarrow \bar{d} + X$	$\sigma_{\text{inv}}/n_{\text{tot}}$	5 to 100 GeV	(any data)
	$p + \text{He} \rightarrow \bar{d} + X$	$\sigma_{\text{inv}}/n_{\text{tot}}$	5 to 100 GeV	(any data)
	$\bar{p} + p \rightarrow \bar{d} + X$	σ_{inv}	2 to 10 GeV	(any data)
$\overline{\text{He}}$	$p + p \rightarrow \overline{\text{He}} + X$	$\sigma_{\text{inv}}/n_{\text{tot}}$	5 to 100 GeV	(any data)
e^{\pm}	$p + \text{He} \rightarrow \pi^{\pm} + X$	σ_{inv}	5 to 100 GeV	$< 5\%$
	$p + \text{He} \rightarrow K^{\pm} + X$			$< 5\%$
γ	$p + p \rightarrow \pi^0 + X$	σ_{inv}	5 to 1000 GeV	$< 5\%$
	$p + \text{He} \rightarrow \pi^0 + X$			$< 5\%$

Measuring production cross sections at accelerators

Uncertainties on cosmic antimatter

D. Maurin, FD et al., 2503.16173

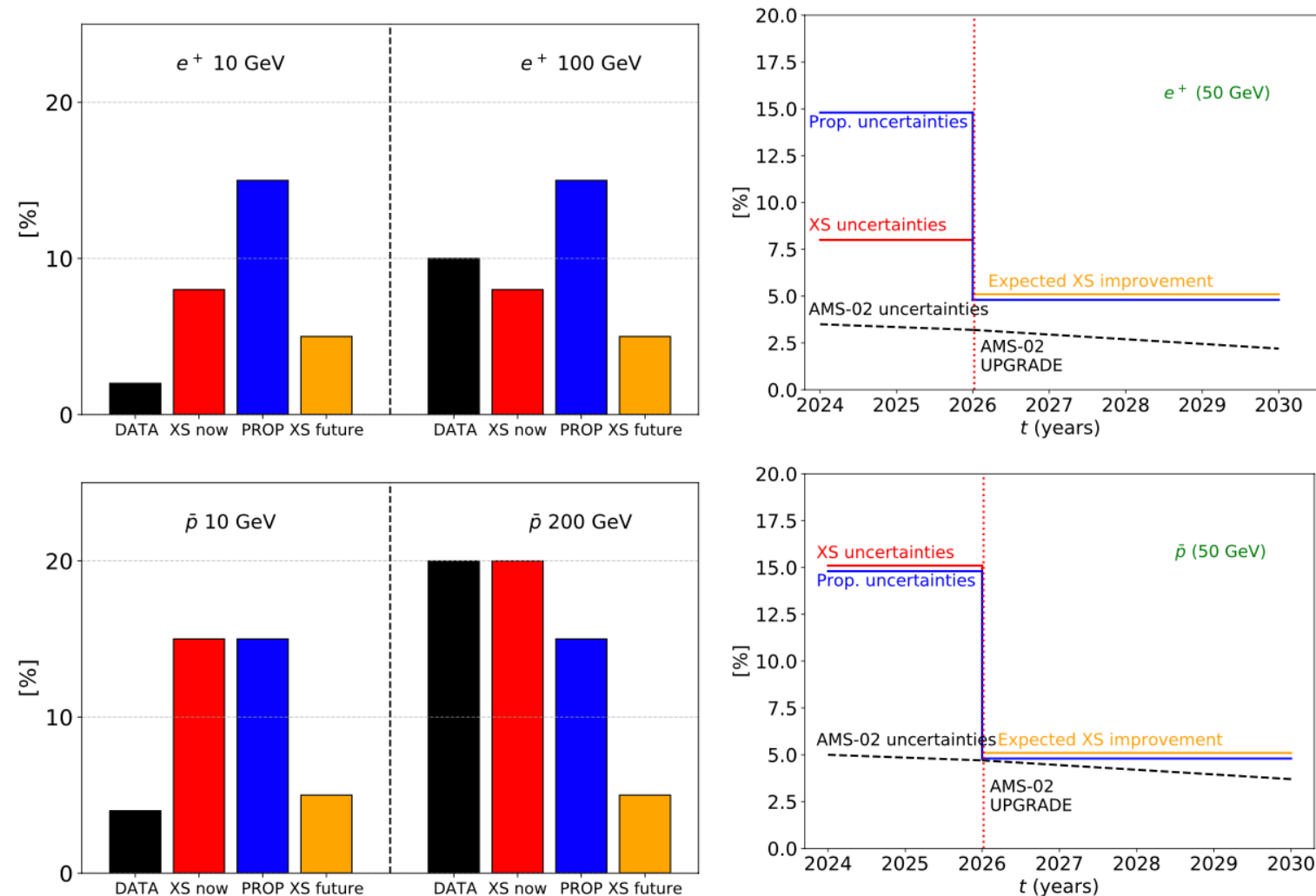


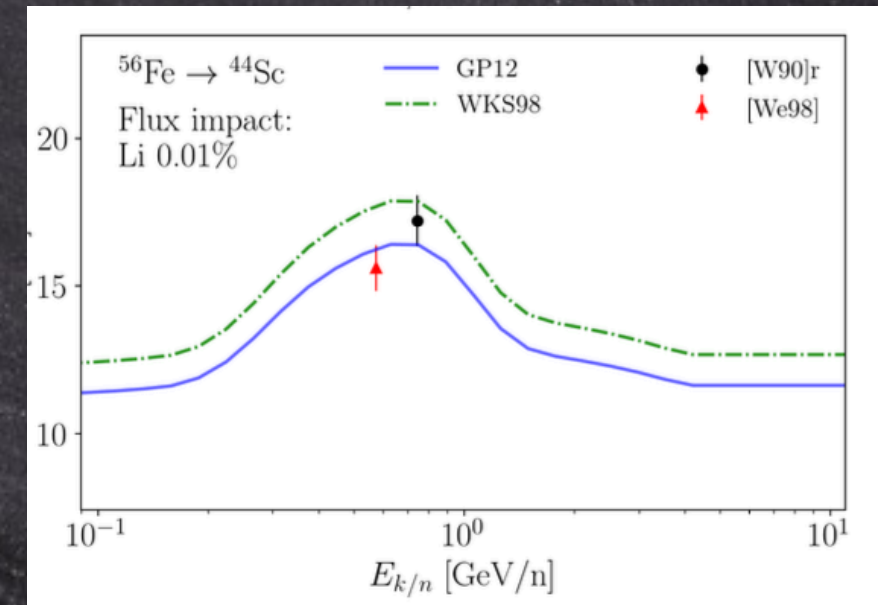
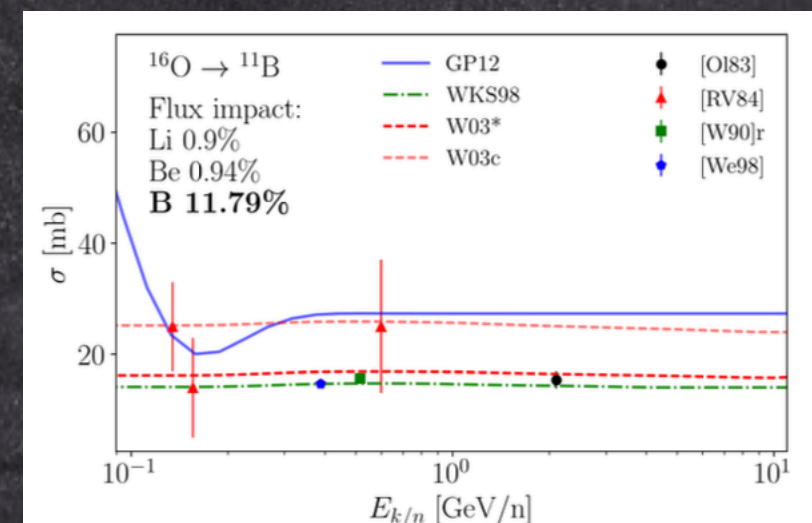
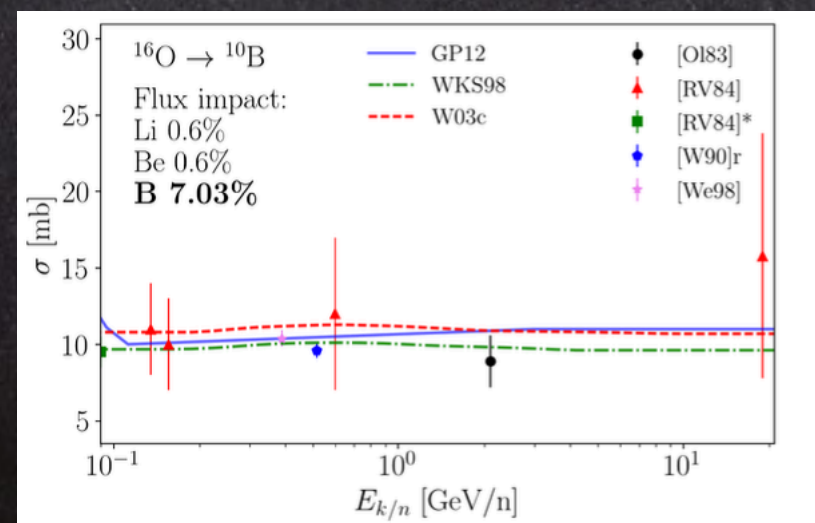
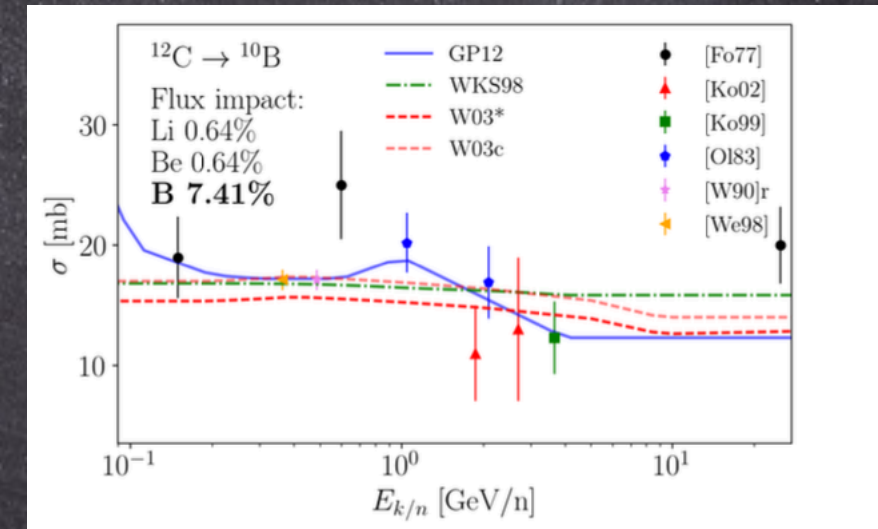
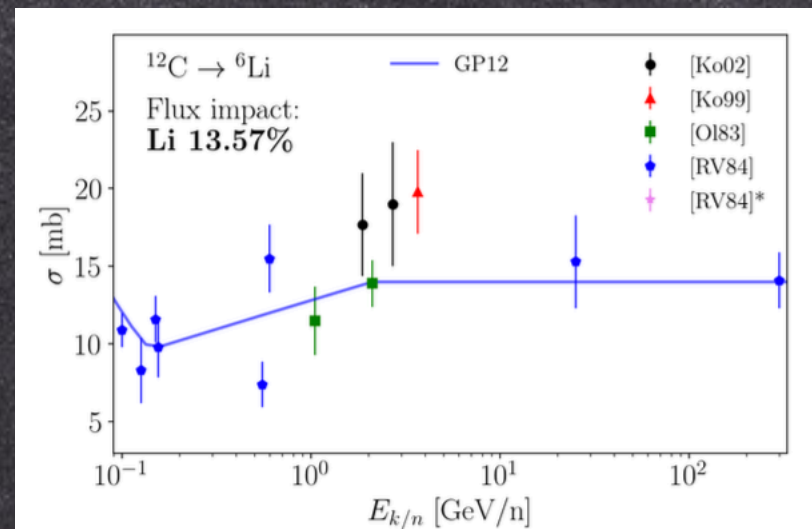
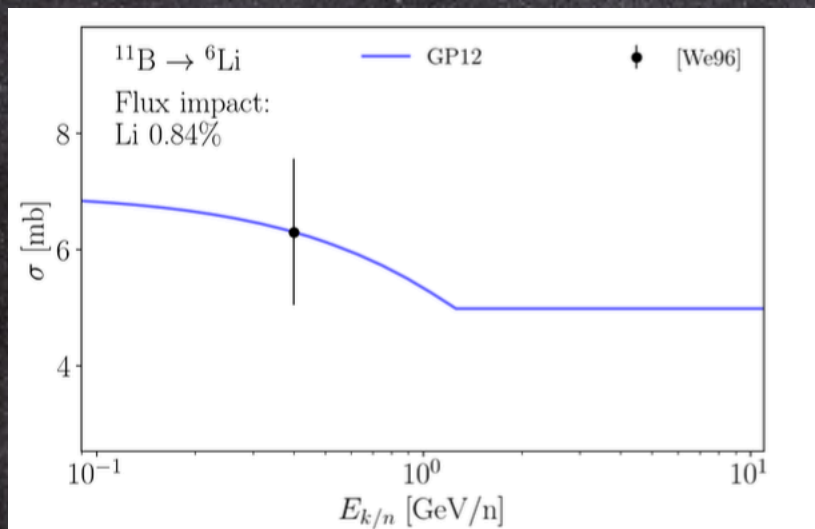
Figure 12: Left: the current AMS experimental \bar{p} errors at 10 and 200 GeV, alongside cross-section and propagation uncertainties. Right: prospects for the future, showing when and how cross-section uncertainties might reach levels comparable to AMS data.

Propagations uncertainties can indirectly be reduced also (not only) by cross section measurements

Cross sections for nuclei CRs

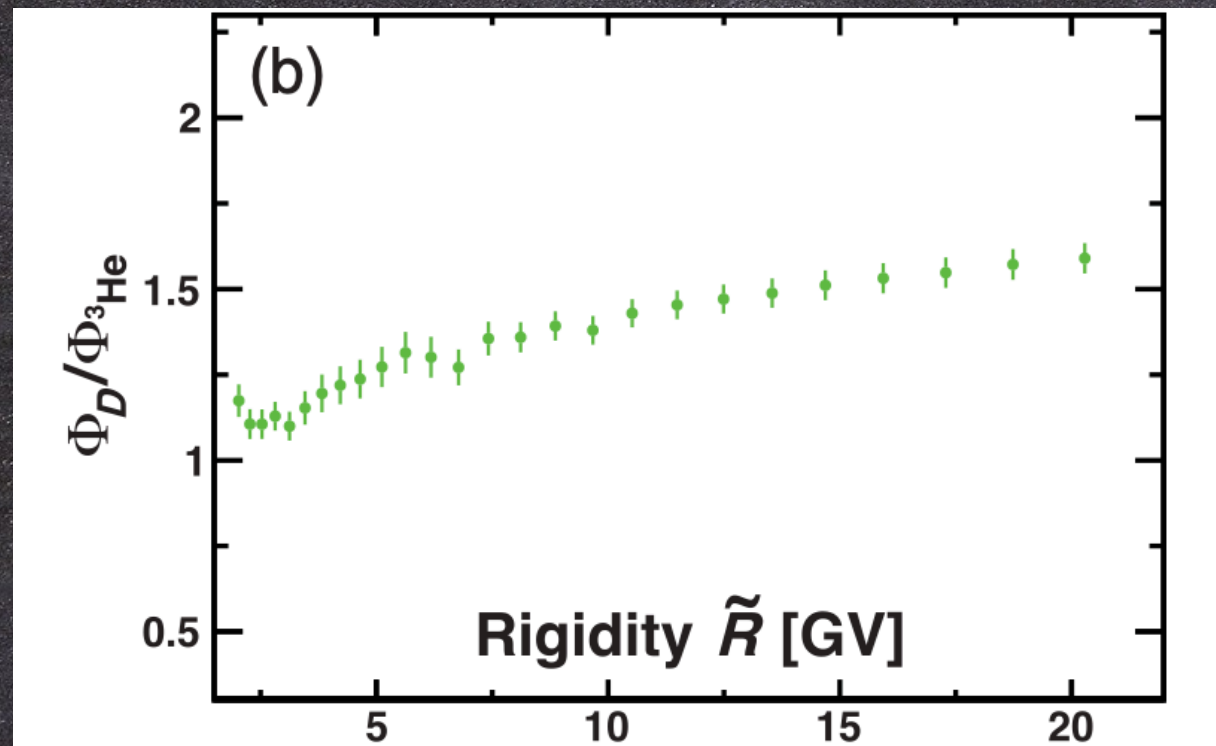
Data driven parameterizations (Silberberg&Tsao), semi-empirical formulae (Webber+), parametric formulae/direct fit to the data (Galprop), MonteCarlo codes (Fluka, Geant, ...)

Genolini, Moskalenko, Maurin, Unger PRC 2018



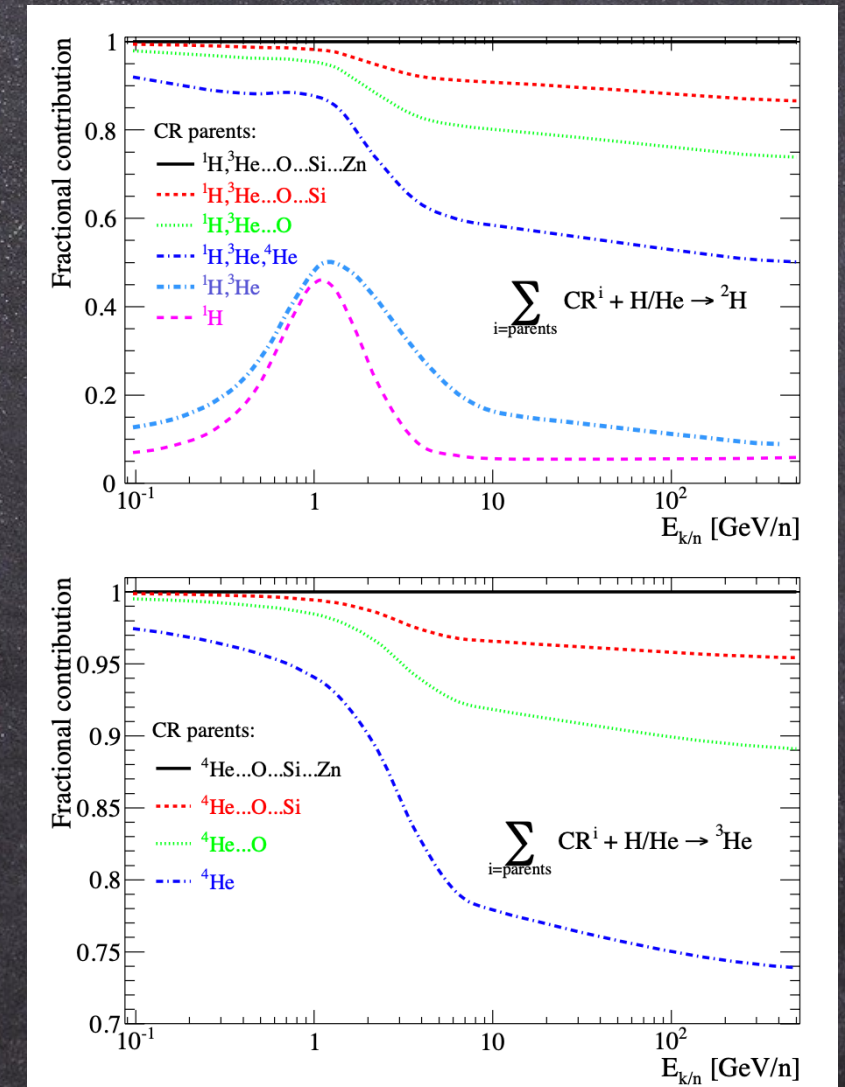
Light isotopes (D, ^3He)

AMS-02 Coll, PRL 2024



D and ^3He do not share identical slopes.
Is there a primary D source?
Uncertainties on XS plague any
further interpretation

Coste+ A&A 2012



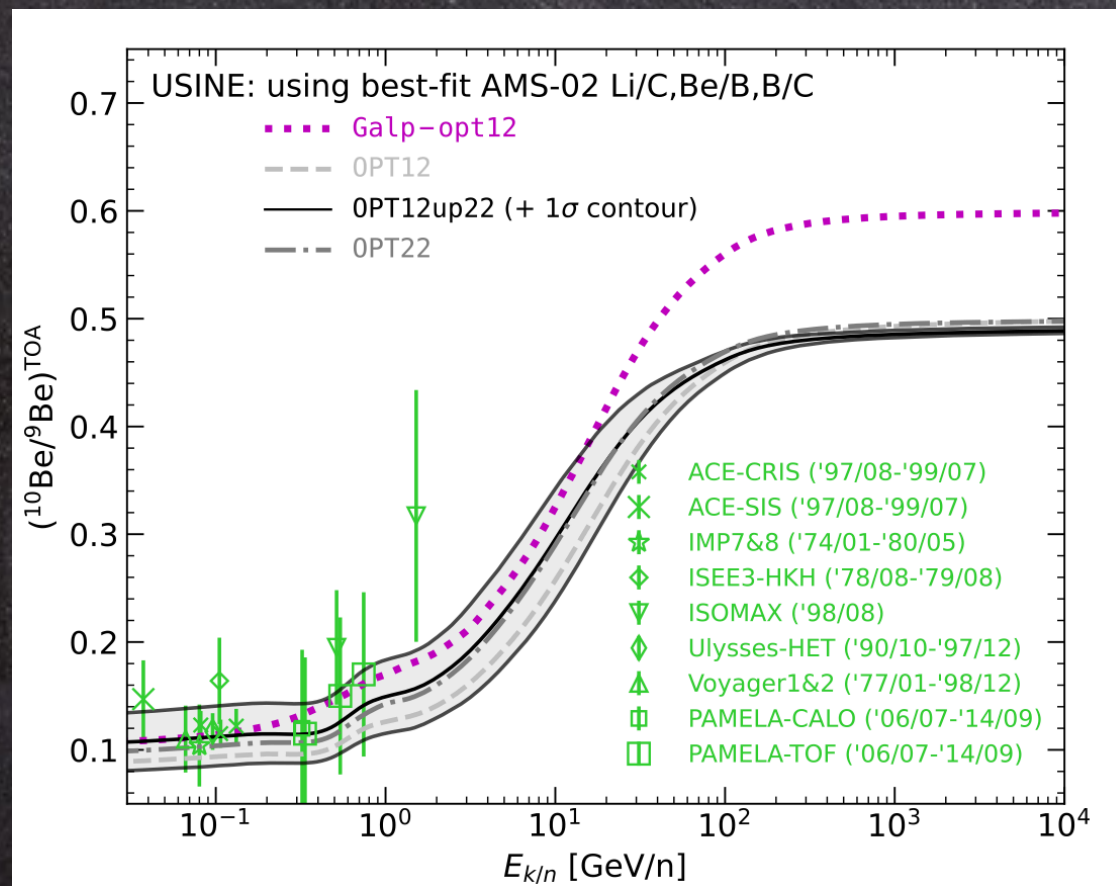
Fractional contribution of
Parent nuclei to D and ^3He
are different

Gomez-Coral+ PRD 2023; Boschini+ ApJ 2025

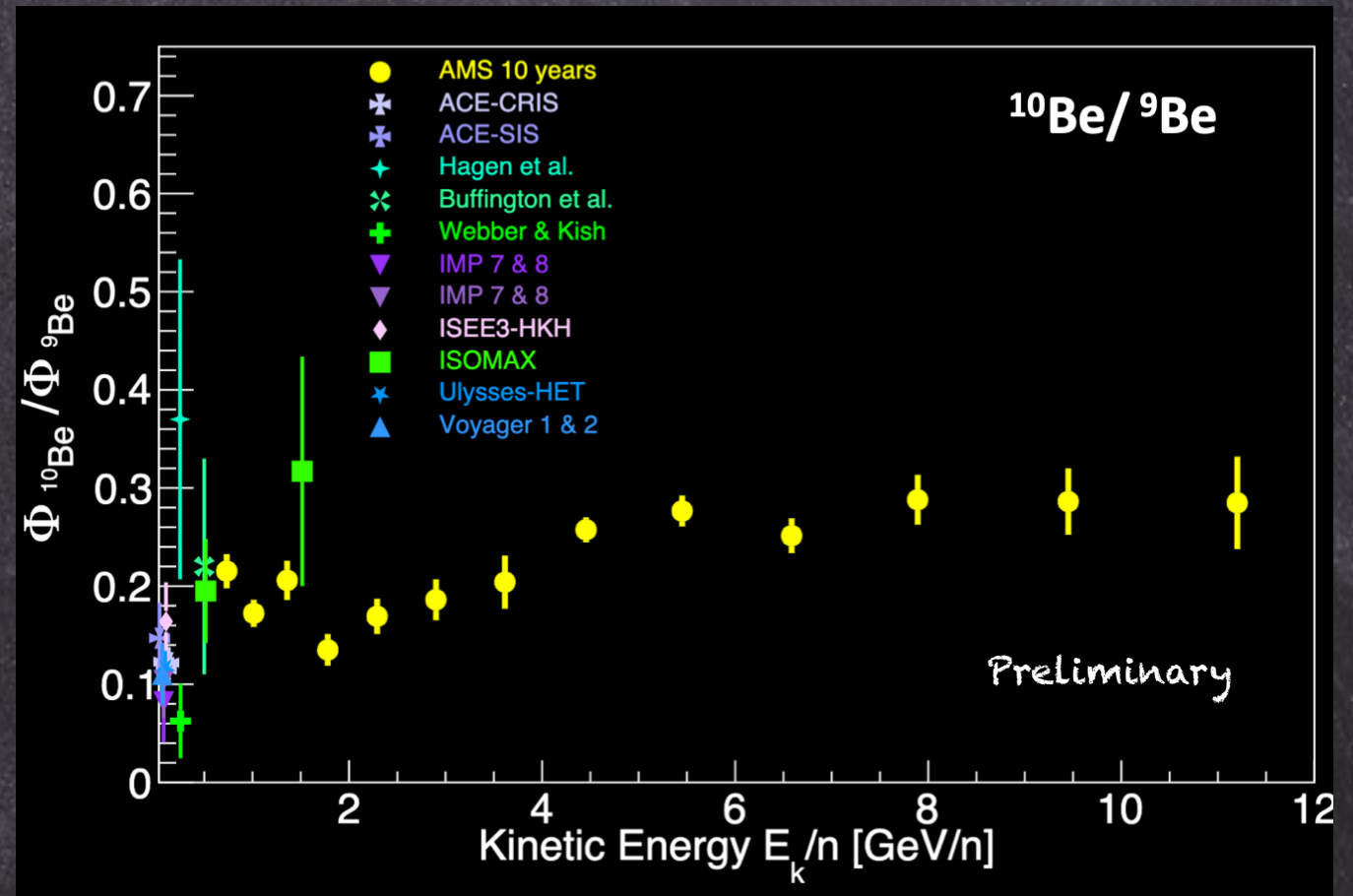
Radioactive Light isotopes

Radioactive isotopes (^{10}Be , ^{26}Al) can track the diffusive halo size
Important to test origin and propagation of CRs

Maurin et al, A&A 2022



AMS Coll. ICRC2023

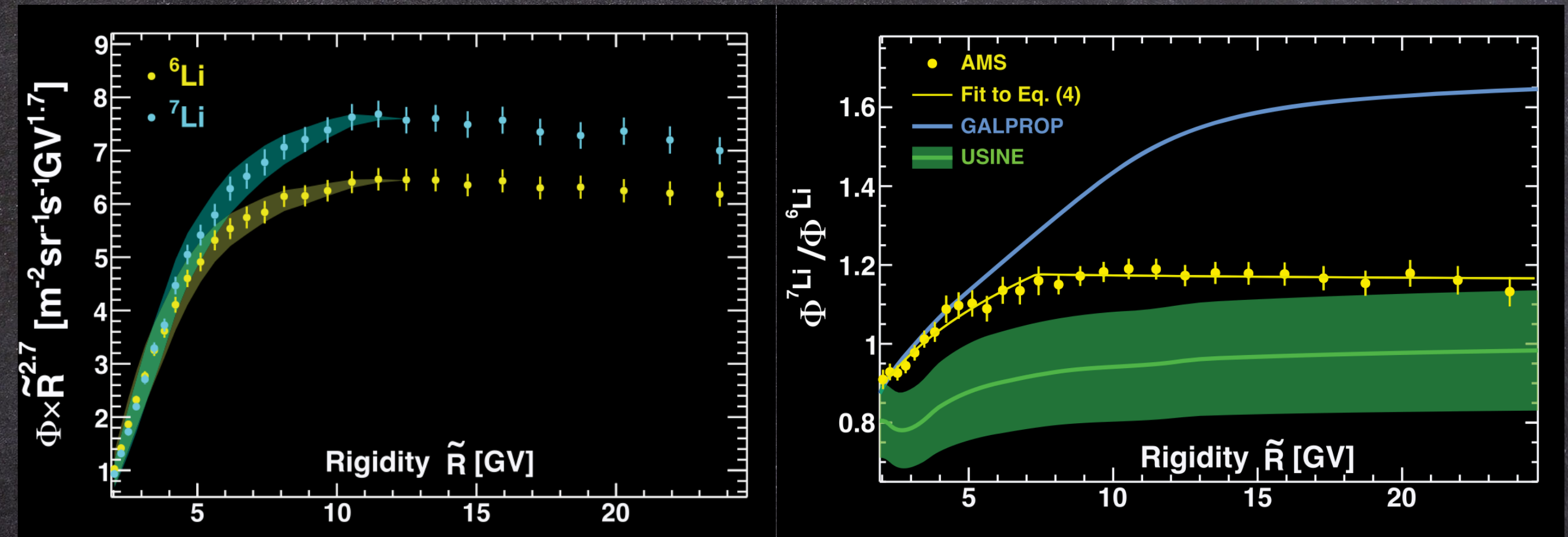


Weinrich et al. A&A 2020 Jacobs, Mertsch, Pahn 2305.10337

Need of precise data on light radioactive isotopes (^{10}Be mainly)
up to 100 GeV/n – and cross sections.

The lithium data: tension with predictions

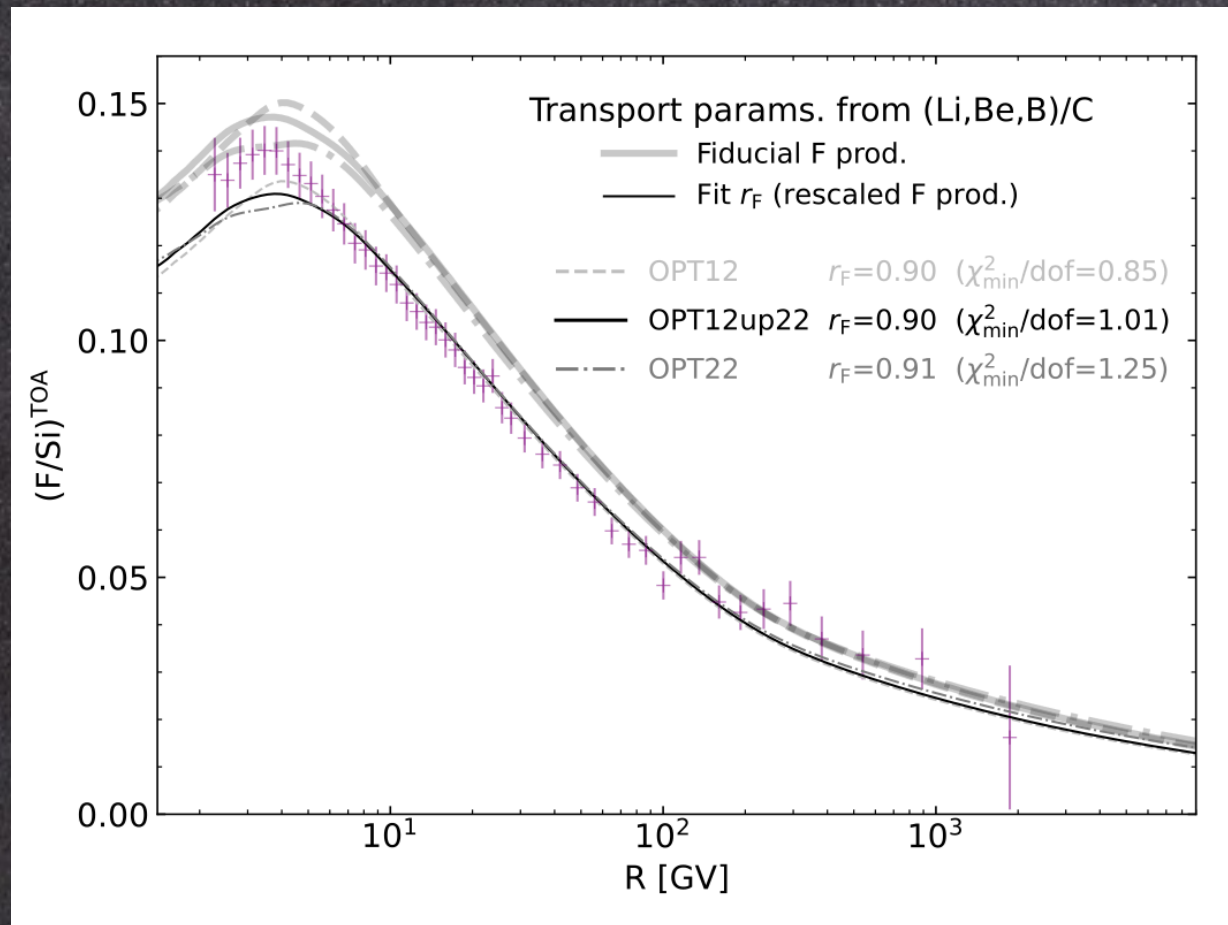
AMS-02 Coll., PRL 2025



${}^6\text{Li}$ and ${}^7\text{Li}$ show the same rigidity behaviour, a primary origin is excluded. Theoretical models do not reproduce the data. Likely a cross section issue

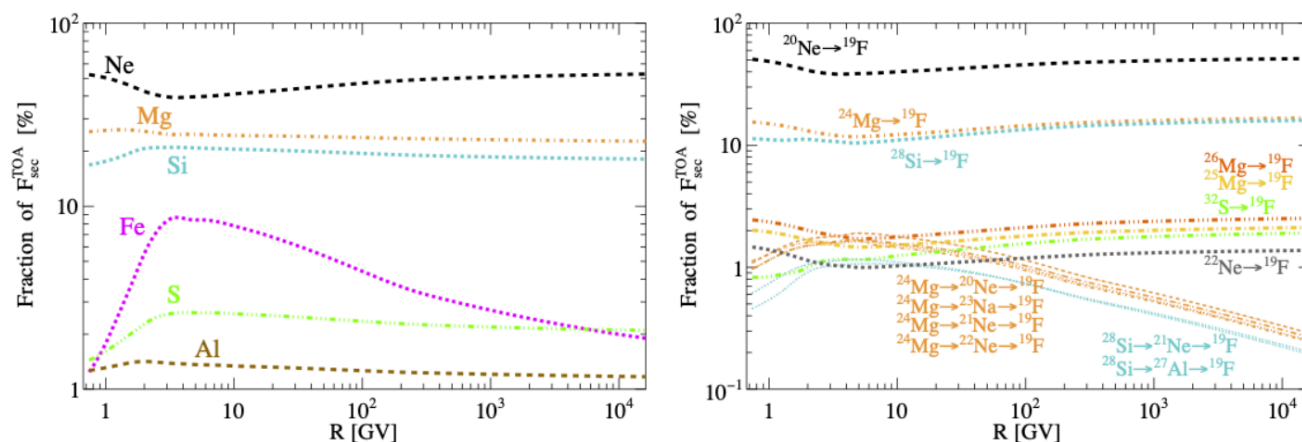
Spallation cross sections for nuclei: the F case

Ferronato Bueno, Derome, Genolini, Maurin, Tatischeff, Vecchi A& 2024



Propagation parameters from lighter nuclei over-predict F/Si measured by AMS-02 (PRL126, 2021).

If cross sections are reduced by 15%, agreement is found for Li to F secondaries



Main progenitors are Ne, Mg, Si, S, Al, and other 35 channels contributing individually [0.1, 2]%, 22% of the total.

Data on cross sections: the state of the art

D. Maurin, FD et al., 2503.16173

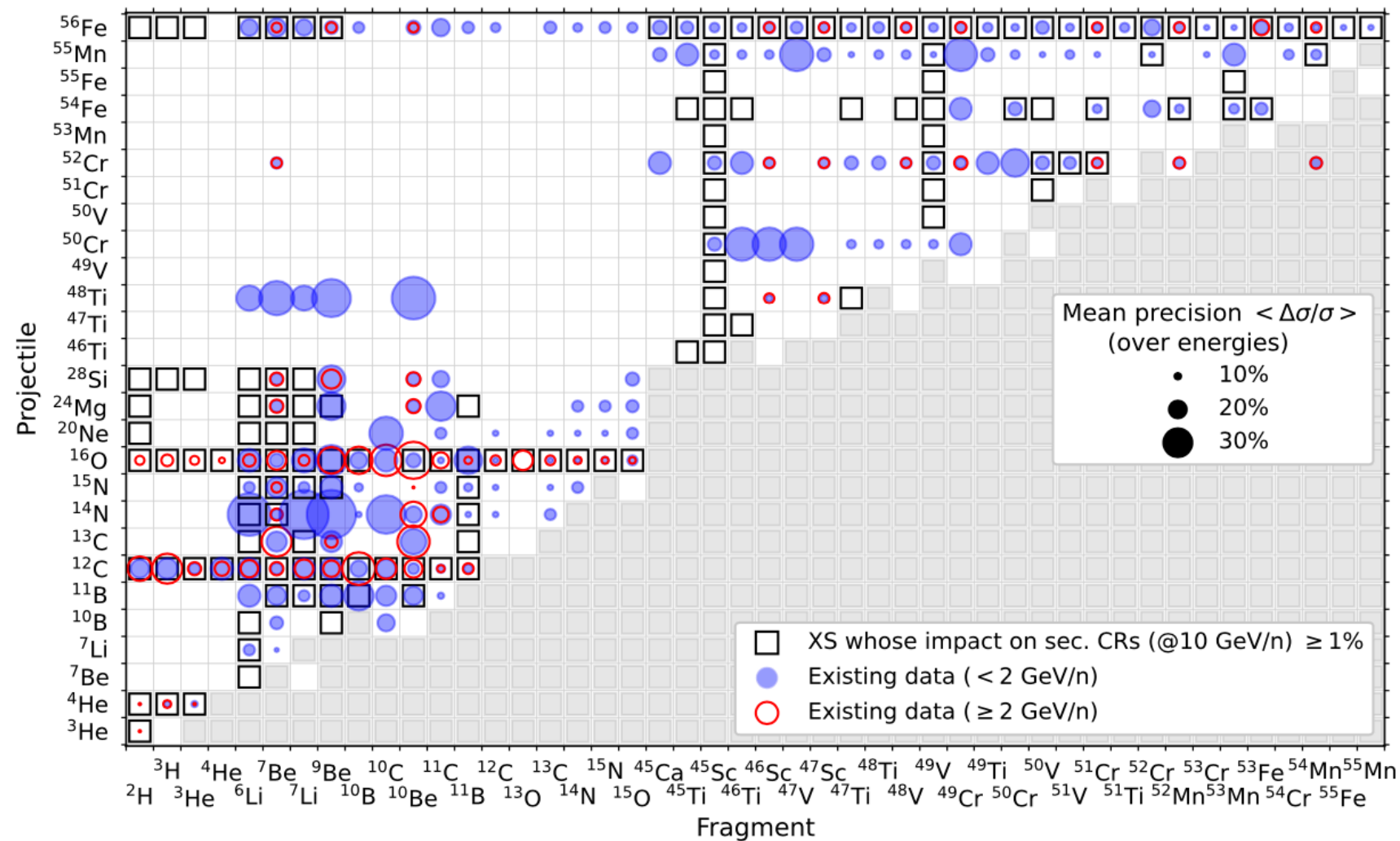


Figure 9: Illustration of the existing nuclear data below (blue disks) and above (red circles) 2 GeV/n, and their relative precision (size of the circles). We restrict ourselves to the matrix of projectiles (y -axis) and fragments (x -axis) formed from the reactions (black empty squares) contributing to at least 1% of the flux of GCR secondary species $Z < 30$, as listed in Table 1). The grey zone shows forbidden production regions ($A_f > A_p$): the fact that some nuclear data are reported for ${}^{52}\text{Cr}$ into ${}^{54}\text{Mn}$, illustrates that some measured cross-sections come from projectiles in natural abundances (i.e., a mix of several isotopes, some heavier than the one reported) instead of single isotopes reported in this figure (for simplicity).

Wish List of individual reactions according to their flux impact

Deuterium		Lithium		Beryllium		Boron		Fluorine	
$^4\text{He} + \text{H} \rightarrow ^2\text{H}$	38.	$^{16}\text{O} + \text{H} \rightarrow ^6\text{Li}$	15.2	$^{16}\text{O} + \text{H} \rightarrow ^7\text{Be}$	16.8	$^{12}\text{C} + \text{H} \rightarrow ^{11}\text{B}$	17.2	$^{20}\text{Ne} + \text{H} \rightarrow ^{19}\text{Ne}$	16.8
$^{16}\text{O} + \text{H} \rightarrow ^2\text{H}$	9.0	$^{12}\text{C} + \text{H} \rightarrow ^6\text{Li}$	12.5	$^{12}\text{C} + \text{H} \rightarrow ^7\text{Be}$	14.5	$^{12}\text{C} + \text{H} \rightarrow ^{11}\text{C}$	16.6	$^{20}\text{Ne} + \text{H} \rightarrow ^{19}\text{F}$	13.9
$^3\text{He} + \text{H} \rightarrow ^2\text{H}$	7.9*	$^{12}\text{C} + \text{H} \rightarrow ^7\text{Li}$	9.93	$^{12}\text{C} + \text{H} \rightarrow ^9\text{Be}$	8.25	$^{16}\text{O} + \text{H} \rightarrow ^{11}\text{B}$	10.8	$^{24}\text{Mg} + \text{H} \rightarrow ^{19}\text{F}$	8.80
$^4\text{He} + \text{He} \rightarrow ^2\text{H}$	6.5	$^{16}\text{O} + \text{H} \rightarrow ^7\text{Li}$	9.74	$^{16}\text{O} + \text{H} \rightarrow ^9\text{Be}$	6.09	$^{16}\text{O} + \text{H} \rightarrow ^{10}\text{B}$	7.85	$^{28}\text{Si} + \text{H} \rightarrow ^{19}\text{F}$	8.12
$^{12}\text{C} + \text{H} \rightarrow ^2\text{H}$	5.8	$^{16}\text{O} + \text{He} \rightarrow ^6\text{Li}$	2.86†	$^{16}\text{O} + \text{He} \rightarrow ^7\text{Be}$	2.87†	$^{12}\text{C} + \text{H} \rightarrow ^{10}\text{B}$	7.05	$^{22}\text{Ne} + \text{H} \rightarrow ^{19}\text{F}$	6.13
$^4\text{He} + \text{H} \rightarrow ^3\text{He}$	5.2	$^{12}\text{C} + \text{H} \rightarrow ^6\text{Li}$	2.14†	$^{12}\text{C} + \text{H} \rightarrow ^{10}\text{Be}$	2.63	$^{16}\text{O} + \text{H} \rightarrow ^{10}\text{B}$	4.42	$^{24}\text{Mg} + \text{H} \rightarrow ^{19}\text{Ne}$	3.48
$^1\text{H} + \text{He} \rightarrow ^2\text{H}$	4.7	$^7\text{Li} + \text{H} \rightarrow ^6\text{Li}$	2.11	$^{24}\text{Mg} + \text{H} \rightarrow ^7\text{Be}$	2.58	$^{16}\text{O} + \text{H} \rightarrow ^{11}\text{C}$	4.12*	$^{56}\text{Fe} + \text{H} \rightarrow ^{19}\text{F}$	3.25
$^{56}\text{Fe} + \text{H} \rightarrow ^2\text{H}$	4.0†	$^{13}\text{C} + \text{H} \rightarrow ^7\text{Li}$	2.05†	$^{14}\text{N} + \text{H} \rightarrow ^7\text{Be}$	2.26	$^{11}\text{B} + \text{H} \rightarrow ^{10}\text{B}$	2.46†	$^{21}\text{Ne} + \text{H} \rightarrow ^{19}\text{F}$	3.17
$^{28}\text{Si} + \text{H} \rightarrow ^2\text{H}$	2.6†	$^{56}\text{Fe} + \text{H} \rightarrow ^7\text{Li}$	2.03	$^{12}\text{C} + \text{He} \rightarrow ^7\text{Be}$	2.26†	$^{16}\text{O} + \text{H} \rightarrow ^{12}\text{C}$	2.45	$^{28}\text{Si} + \text{H} \rightarrow ^{19}\text{Ne}$	2.99
$^{24}\text{Mg} + \text{H} \rightarrow ^2\text{H}$	2.1†	$^{15}\text{N} + \text{H} \rightarrow ^7\text{Li}$	1.95	$^{11}\text{B} + \text{H} \rightarrow ^9\text{Be}$	2.22	$^{15}\text{N} + \text{H} \rightarrow ^{11}\text{B}$	2.25	$^{23}\text{Na} + \text{H} \rightarrow ^{19}\text{F}$	2.30
$^{16}\text{O} + \text{He} \rightarrow ^2\text{H}$	1.5	$^{16}\text{O} + \text{H} \rightarrow ^{15}\text{N}$	1.88	$^{16}\text{O} + \text{H} \rightarrow ^{10}\text{Be}$	1.69	$^{12}\text{C} + \text{He} \rightarrow ^{11}\text{C}$	2.20†	$^{25}\text{Mg} + \text{H} \rightarrow ^{19}\text{F}$	2.24*
$^{20}\text{Ne} + \text{H} \rightarrow ^2\text{H}$	1.2†	$^{16}\text{O} + \text{He} \rightarrow ^6\text{Li}$	1.82†	$^{20}\text{Ne} + \text{H} \rightarrow ^7\text{Be}$	1.67†	$^{16}\text{O} + \text{H} \rightarrow ^{15}\text{N}$	1.84	$^{26}\text{Mg} + \text{H} \rightarrow ^{19}\text{F}$	2.19
$^{16}\text{O} + \text{H} \rightarrow ^{15}\text{N}$	1.1	$^{56}\text{Fe} + \text{H} \rightarrow ^6\text{Li}$	1.74	$^{56}\text{Fe} + \text{H} \rightarrow ^7\text{Be}$	1.66*	$^{16}\text{O} + \text{He} \rightarrow ^{11}\text{B}$	1.66†	$^{20}\text{Ne} + \text{He} \rightarrow ^{19}\text{Ne}$	1.97†
		$^{12}\text{C} + \text{He} \rightarrow ^7\text{Li}$	1.71†*	$^{16}\text{O} + \text{H} \rightarrow ^{12}\text{C}$	1.61	$^{16}\text{O} + \text{H} \rightarrow ^{15}\text{O}$	1.64	$^{27}\text{Al} + \text{H} \rightarrow ^{19}\text{F}$	1.73†
		$^{16}\text{O} + \text{H} \rightarrow ^{13}\text{O}$	1.70	$^{16}\text{O} + \text{H} \rightarrow ^{12}\text{C}$	1.53†	$^{16}\text{O} + \text{H} \rightarrow ^{11}\text{B}$	1.64	$^{24}\text{Mg} + \text{H} \rightarrow ^{20}\text{Ne}$	1.36
		$^{24}\text{Mg} + \text{H} \rightarrow ^6\text{Li}$	1.69†	$^{24}\text{Mg} + \text{H} \rightarrow ^9\text{Be}$	1.52	$^{14}\text{N} + \text{H} \rightarrow ^{11}\text{B}$	1.52†	$^{22}\text{Ne} + \text{H} \rightarrow ^{19}\text{O}$	1.29
		$^{28}\text{Si} + \text{H} \rightarrow ^6\text{Li}$	1.69†	$^{16}\text{O} + \text{H} \rightarrow ^{15}\text{N}$	1.41	$^{13}\text{C} + \text{H} \rightarrow ^{11}\text{B}$	1.45	$^{28}\text{Si} + \text{He} \rightarrow ^{19}\text{F}$	1.21†
		$^{13}\text{C} + \text{H} \rightarrow ^{13}\text{O}$	1.68†	$^{56}\text{Fe} + \text{H} \rightarrow ^9\text{Be}$	1.33	$^{12}\text{C} + \text{H} \rightarrow ^{10}\text{C}$	1.32	$^{24}\text{Mg} + \text{He} \rightarrow ^{19}\text{F}$	1.19†
		$^{16}\text{O} + \text{H} \rightarrow ^{12}\text{C}$	1.68	$^{12}\text{C} + \text{H} \rightarrow ^{11}\text{B}$	1.29†	$^{16}\text{O} + \text{H} \rightarrow ^{14}\text{N}$	1.31	$^{24}\text{Mg} + \text{H} \rightarrow ^{21}\text{Ne}$	1.08
		$^{16}\text{O} + \text{H} \rightarrow ^{12}\text{C}$	1.51	$^{12}\text{C} + \text{H} \rightarrow ^{11}\text{B}$	1.28	$^{12}\text{C} + \text{H} \rightarrow ^{10}\text{Be}$	1.16	$^{24}\text{Mg} + \text{H} \rightarrow ^{23}\text{Na}$	1.08
		$^{24}\text{Mg} + \text{H} \rightarrow ^7\text{Li}$	1.50†	$^{16}\text{O} + \text{H} \rightarrow ^{15}\text{O}$	1.26	$^{16}\text{O} + \text{H} \rightarrow ^{10}\text{B}$	1.12†	$^{28}\text{Si} + \text{H} \rightarrow ^{27}\text{Al}$	1.05
		$^{28}\text{Si} + \text{H} \rightarrow ^7\text{Li}$	1.50†	$^{12}\text{C} + \text{H} \rightarrow ^{11}\text{C}$	1.24	$^{16}\text{O} + \text{H} \rightarrow ^{10}\text{B}$	1.10†	$^{56}\text{Fe} + \text{H} \rightarrow ^{19}\text{F}$	1.03†
		$^{10}\text{B} + \text{H} \rightarrow ^6\text{Li}$	1.41†	$^{15}\text{N} + \text{H} \rightarrow ^9\text{Be}$	1.22	$^{24}\text{Mg} + \text{H} \rightarrow ^{11}\text{B}$	1.01†	$^{21}\text{Ne} + \text{H} \rightarrow ^{19}\text{Ne}$	1.03†
		$^{14}\text{N} + \text{H} \rightarrow ^6\text{Li}$	1.39	$^{16}\text{O} + \text{H} \rightarrow ^{14}\text{N}$	1.20				
		$^{15}\text{N} + \text{H} \rightarrow ^6\text{Li}$	1.37	$^{11}\text{B} + \text{H} \rightarrow ^{10}\text{Be}$	1.10				
		$^{16}\text{O} + \text{H} \rightarrow ^{14}\text{N}$	1.27	$^{15}\text{N} + \text{H} \rightarrow ^7\text{Be}$	1.08				
		$^{20}\text{Ne} + \text{H} \rightarrow ^6\text{Li}$	1.16†	$^{16}\text{O} + \text{H} \rightarrow ^{13}\text{O}$	1.08				
		$^{12}\text{C} + \text{H} \rightarrow ^{11}\text{B}$	1.15	$^{16}\text{O} + \text{He} \rightarrow ^9\text{Be}$	1.05†				
		$^7\text{Be} + \text{H} \rightarrow ^6\text{Li}$	1.14†	$^{11}\text{B} + \text{H} \rightarrow ^7\text{Be}$	1.04				
		$^{12}\text{C} + \text{H} \rightarrow ^{11}\text{C}$	1.11						
		$^{16}\text{O} + \text{H} \rightarrow ^{13}\text{C}$	1.10						
		$^{20}\text{Ne} + \text{H} \rightarrow ^7\text{Li}$	1.02†						
Scandium		Titanium		Vanadium		Chromium		Manganese	
$^{56}\text{Fe} + \text{H} \rightarrow ^{45}\text{Sc}$	43.9	$^{56}\text{Fe} + \text{H} \rightarrow ^{47}\text{Ti}$	17.3	$^{56}\text{Fe} + \text{H} \rightarrow ^{49}\text{V}$	30.7	$^{56}\text{Fe} + \text{H} \rightarrow ^{52}\text{Cr}$	22.7	$^{56}\text{Fe} + \text{H} \rightarrow ^{53}\text{Mn}$	30.2
$^{56}\text{Fe} + \text{H} \rightarrow ^{45}\text{Ti}$	6.35*	$^{56}\text{Fe} + \text{H} \rightarrow ^{48}\text{Ti}$	11.1	$^{56}\text{Fe} + \text{H} \rightarrow ^{50}\text{V}$	22.3*	$^{56}\text{Fe} + \text{H} \rightarrow ^{51}\text{Cr}$	21.2	$^{56}\text{Fe} + \text{H} \rightarrow ^{55}\text{Mn}$	27.2*
$^{56}\text{Fe} + \text{He} \rightarrow ^{45}\text{Sc}$	4.95†	$^{56}\text{Fe} + \text{H} \rightarrow ^{46}\text{Ti}$	10.5	$^{56}\text{Fe} + \text{H} \rightarrow ^{51}\text{Ti}$	5.66	$^{56}\text{Fe} + \text{H} \rightarrow ^{50}\text{Cr}$	12.9*	$^{56}\text{Fe} + \text{H} \rightarrow ^{54}\text{Mn}$	18.6
$^{56}\text{Fe} + \text{H} \rightarrow ^{45}\text{Ca}$	3.27	$^{56}\text{Fe} + \text{H} \rightarrow ^{48}\text{V}$	8.71	$^{56}\text{Fe} + \text{H} \rightarrow ^{49}\text{V}$	3.93	$^{56}\text{Fe} + \text{H} \rightarrow ^{53}\text{Cr}$	5.96	$^{54}\text{Fe} + \text{H} \rightarrow ^{53}\text{Mn}$	4.78
$^{47}\text{Ti} + \text{H} \rightarrow ^{45}\text{Sc}$	3.24†	$^{56}\text{Fe} + \text{H} \rightarrow ^{46}\text{Sc}$	4.34*	$^{56}\text{Fe} + \text{H} \rightarrow ^{49}\text{Cr}$	3.26	$^{56}\text{Fe} + \text{H} \rightarrow ^{52}\text{Mn}$	4.08	$^{56}\text{Fe} + \text{He} \rightarrow ^{53}\text{Mn}$	4.00†
$^{54}\text{Fe} + \text{H} \rightarrow ^{45}\text{Sc}$	3.07†	$^{56}\text{Fe} + \text{H} \rightarrow ^{49}\text{Ti}$	3.36	$^{56}\text{Fe} + \text{H} \rightarrow ^{52}\text{Cr}$	2.77	$^{56}\text{Fe} + \text{H} \rightarrow ^{55}\text{Fe}$	3.11	$^{56}\text{Fe} + \text{He} \rightarrow ^{55}\text{Mn}$	3.62†
$^{56}\text{Fe} + \text{H} \rightarrow ^{55}\text{Fe}$	2.76	$^{56}\text{Fe} + \text{H} \rightarrow ^{55}\text{Fe}$	2.80	$^{56}\text{Fe} + \text{H} \rightarrow ^{50}\text{V}$	2.61†	$^{56}\text{Fe} + \text{He} \rightarrow ^{52}\text{Cr}$	2.81†	$^{54}\text{Fe} + \text{H} \rightarrow ^{53}\text{Mn}$	3.06
$^{56}\text{Fe} + \text{H} \rightarrow ^{47}\text{Ti}$	2.63	$^{56}\text{Fe} + \text{H} \rightarrow ^{49}\text{V}$	2.63	$^{56}\text{Fe} + \text{H} \rightarrow ^{51}\text{Cr}$	2.58†	$^{56}\text{Fe} + \text{H} \rightarrow ^{53}\text{Mn}$	2.59	$^{56}\text{Fe} + \text{He} \rightarrow ^{53}\text{Fe}$	2.64
$^{46}\text{Ti} + \text{H} \rightarrow ^{45}\text{Sc}$	2.51†	$^{56}\text{Fe} + \text{H} \rightarrow ^{51}\text{Cr}$	2.08	$^{56}\text{Fe} + \text{H} \rightarrow ^{54}\text{Mn}$	1.79	$^{56}\text{Fe} + \text{H} \rightarrow ^{54}\text{Mn}$	2.23	$^{56}\text{Fe} + \text{H} \rightarrow ^{54}\text{Mn}$	2.47†
$^{48}\text{Ti} + \text{H} \rightarrow ^{45}\text{Sc}$	2.45†	$^{56}\text{Fe} + \text{H} \rightarrow ^{54}\text{Mn}$	2.02	$^{56}\text{Fe} + \text{H} \rightarrow ^{50}\text{V}$	1.72	$^{54}\text{Fe} + \text{H} \rightarrow ^{53}\text{Mn}$	1.96	$^{56}\text{Fe} + \text{He} \rightarrow ^{55}\text{Fe}$	2.33
$^{46}\text{Ti} + \text{H} \rightarrow ^{45}\text{Ti}$	2.24†	$^{56}\text{Fe} + \text{H} \rightarrow ^{47}\text{Ti}$	1.94†	$^{56}\text{Fe} + \text{H} \rightarrow ^{51}\text{V}$	1.69	$^{56}\text{Fe} + \text{H} \rightarrow ^{50}\text{Cr}$	1.88	$^{55}\text{Fe} + \text{H} \rightarrow ^{53}\text{Mn}$	1.30†
$^{52}\text{Cr} + \text{H} \rightarrow ^{45}\text{Sc}$	2.02	$^{56}\text{Fe} + \text{H} \rightarrow ^{53}\text{Mn}$	1.93	$^{56}\text{Fe} + \text{H} \rightarrow ^{55}\text{Mn}$	1.59	$^{56}\text{Fe} + \text{H} \rightarrow ^{51}\text{Cr}$	1.62	$^{55}\text{Mn} + \text{H} \rightarrow ^{54}\text{Mn}$	1.03
$^{56}\text{Fe} + \text{H} \rightarrow ^{49}\text{V}$	2.02	$^{56}\text{Fe} + \text{H} \rightarrow ^{47}\text{V}$	1.93	$^{56}\text{Fe} + \text{H} \rightarrow ^{50}\text{V}$	1.34	$^{56}\text{Fe} + \text{H} \rightarrow ^{50}\text{Cr}$	1.59†		
$^{56}\text{Fe} + \text{H} \rightarrow ^{46}\text{Ti}$	1.98	$^{56}\text{Fe} + \text{H} \rightarrow ^{52}\text{Cr}$	1.86	$^{56}\text{Fe} + \text{H} \rightarrow ^{51}\text{V}$	1.30†	$^{54}\text{Fe} + \text{H} \rightarrow ^{50}\text{Cr}$	1.21		
$^{56}\text{Fe} + \text{H} \rightarrow ^{52}\text{Cr}$	1.93	$^{56}\text{Fe} + \text{H} \rightarrow ^{47}\text{Sc}$	1.75	$^{56}\text{Fe} + \text{H} \rightarrow ^{53}\text{Mn}$	1.23†	$^{55}\text{Mn} + \text{H} \rightarrow$	1.11		
$^{56}\text{Fe} + \text{H} \rightarrow ^{51}\text{Cr}$	1.93	$^{56}\text{Fe} + \text{H} \rightarrow ^{50}\text{V}$	1.70	$^{56}\text{Fe} + \text{H} \rightarrow ^{54}\text{Mn}$	1.18†				
$^{56}\text{Fe} + \text{H} \rightarrow ^{54}\text{Mn}$	1.91	$^{56}\text{Fe} + \text{H} \rightarrow ^{55}\text{Mn}$	1.53	$^{56}\text{Fe} + \text{H} \rightarrow ^{55}\text{Mn}$	1.14†				
$^{49}\text{V} + \text{H} \rightarrow ^{45}\text{Sc}$	1.90†	$^{54}\text{Fe} + \text{H} \rightarrow ^{46}\text{Ti}$	1.36†	$^{56}\text{Fe} + \text{H} \rightarrow ^{50}\text{Cr}$	1.07†				
$^{54}\text{Fe} + \text{H} \rightarrow ^{45}\text{Ti}$	1.84†	$^{54}\text{Fe} + \text{H} \rightarrow ^{48}\text{V}$	1.33†	$^{56}\text{Fe} + \text{H} \rightarrow ^{51}\text{V}$	1.03				
$^{56}\text{Fe} + \text{H} \rightarrow ^{53}\text{Mn}$	1.79	$^{54}\text{Fe} + \text{H} \rightarrow ^{47}\text{Ti}$	1.29†	$^{56}\text{Fe} + \text{H} \rightarrow ^{52}\text{Cr}$	1.01†				
$^{56}\text{Fe} + \text{H} \rightarrow ^{55}\text{Mn}$	1.53	$^{56}\text{Fe} + \text{H} \rightarrow ^{50}\text{Cr}$	1.25						
$^{51}\text{Cr} + \text{H} \rightarrow ^{45}\text{Sc}$	1.49†	$^{56}\text{Fe} + \text{He} \rightarrow ^{48}\text{Ti}$	1.24†						
$^{55}\text{Mn} + \text{H} \rightarrow ^{45}\text{Sc}$	1.47	$^{48}\text{Ti} + \text{H} \rightarrow ^{47}\text{Ti}$	1.23†						
$^{55}\text{Fe} + \text{H} \rightarrow ^{45}\text{Sc}$	1.40†	$^{56}\text{Fe} + \text{He} \rightarrow ^{46}\text{Ti}$	1.17†						
$^{56}\text{Fe} + \text{H} \rightarrow ^{50}\text{V}$	1.32	$^{47}\text{Ti} + \text{H} \rightarrow ^{46}\text{Ti}$	1.09†						
$^{56}\text{Fe} + \text{H} \rightarrow ^{50}\text{Cr}$	1.30	$^{56}\text{Fe} + \text{He} \rightarrow ^{48}\text{V}$	1.02†						
$^{53}\text{Mn} + \text{H} \rightarrow ^{45}\text{Sc}$	1.25†								
$^{56}\text{Fe} + \text{H} \rightarrow ^{48}\text{Ti}$	1.22								
$^{50}\text{V} + \text{H} \rightarrow ^{45}\text{Sc}$	1.11†								
$^{50}\text{Cr} + \text{H} \rightarrow ^{45}\text{Sc}$	1.00								

CR secondaries at 10.6 GeV/n

Several reactions have
inconsistent data,
or 1 or 2 points only

Elaborated from:
Genolini+ PRC 2018; 2024

Envisaged energies

Message zero: any new data is welcome, and will bring improvement.

Then, campaigns should be foreseen.

1. high-precision measurement ($\leq 1\%$) of a few specific production cross-sections over the energy range $\sim 0.1-10 \text{ GeV/n}$
2. high-precision measurement of all fragments of many reactions at once at a unique energy

Trying a practical ranking

The most relevant progenitors in GCRs (thus the beam) are:

^1H , ^4He , ^{12}C , ^{16}O , ^{20}Ne , ^{24}Mg , ^{28}Si , ^{56}Fe

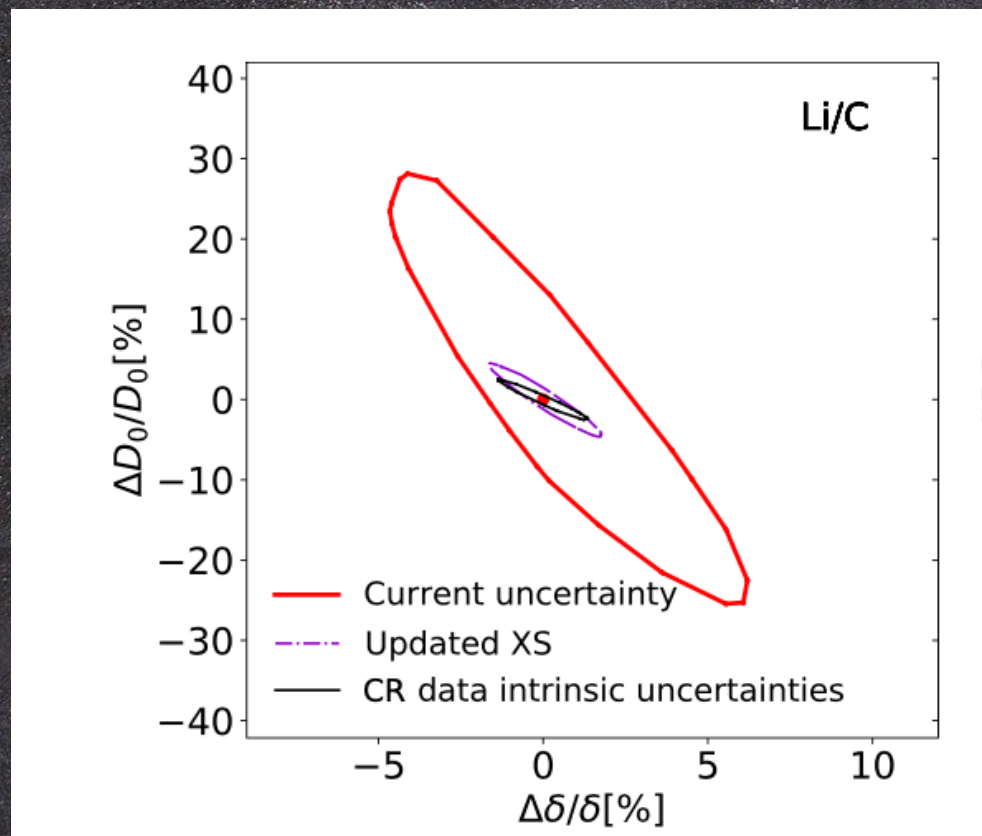
The interstellar medium (thus the target) is made by:

90% H and 10% He

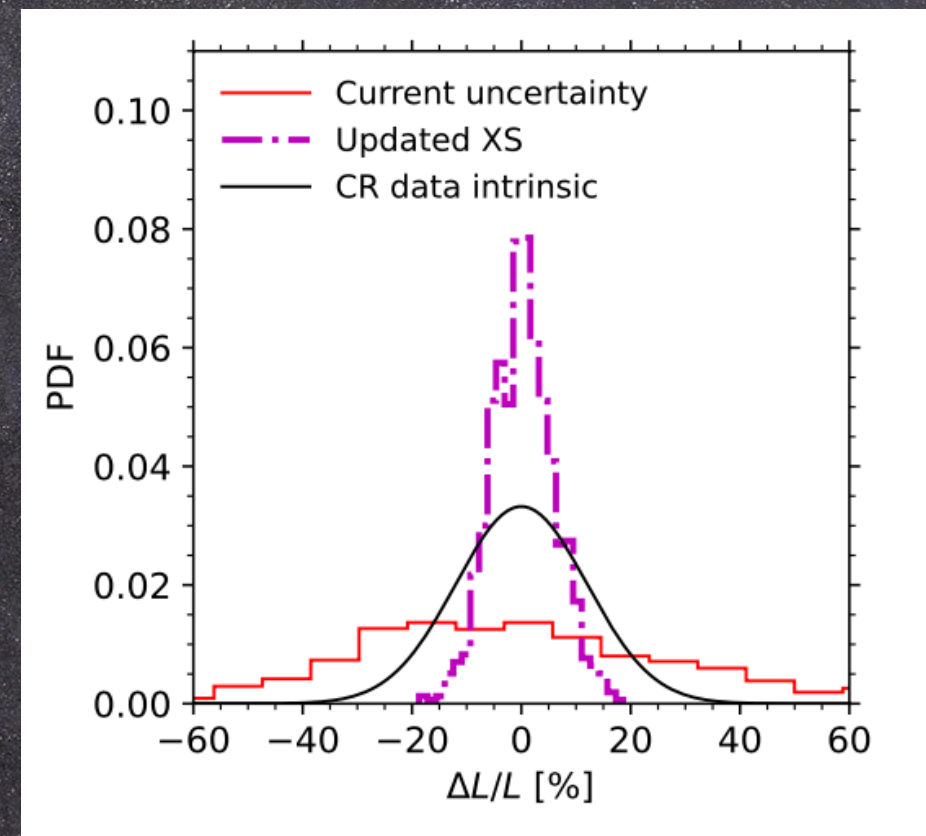
Table 2: Required number of interactions to be recorded, ordered by increasing charge and mass of the projectiles, in order to reach a modelling precision $\lesssim 1\%$ on [GCR](#) fluxes Li, Be, B and F. Adapted from Table IV of Ref. [\[207\]](#).

Reaction	N_{int}	Reaction	N_{int}	Reaction	N_{int}
$^7\text{Li}+\text{H}$	5k	$^{20}\text{Ne}+\text{H}$	50k	$^{28}\text{Si}+\text{H}$	50k
$^{10}\text{B}+\text{H}$	5k	$^{20}\text{Ne}+\text{He}$	10k	$^{28}\text{Si}+\text{He}$	10k
$^{11}\text{B}+\text{H}$	10k	$^{21}\text{Ne}+\text{H}$	10k	$^{29}\text{Si}+\text{H}$	5k
$^{12}\text{C}+\text{H}$	50k	$^{22}\text{Ne}+\text{H}$	20k	$^{32}\text{S}+\text{H}$	5k
$^{12}\text{C}+\text{He}$	10k	$^{22}\text{Ne}+\text{He}$	5k	$^{56}\text{Fe}+\text{H}$	30k
$^{13}\text{C}+\text{H}$	5k	$^{23}\text{Na}+\text{H}$	10k	$^{56}\text{Fe}+\text{He}$	10k
$^{14}\text{N}+\text{H}$	10k	$^{24}\text{Mg}+\text{H}$	50k		
$^{15}\text{N}+\text{H}$	10k	$^{24}\text{Mg}+\text{He}$	10k		
$^{16}\text{O}+\text{H}$	60k	$^{25}\text{Mg}+\text{H}$	10k		
$^{16}\text{O}+\text{He}$	20k	$^{26}\text{Mg}+\text{H}$	10k		
		$^{27}\text{Al}+\text{H}$	10k		

Forecast of the impact of new XS measurements on Galactic propagation



normalisation and slope of the spatial diffusion coefficient entering the GCR transport



diffusive halo size determination

Forecast performed with previous indications of $<1\%$ precision on the fluxes of Li, Be, B, F.

These improvements reflect on all the CR predictions

Main facilities and experiments for ongoing and future cross-section measurements - I

At the LHC:

- **LHCb**, operated in **fixed-target mode** by using SMOG

\sqrt{s} : 27 - 113 GeV (E_{lab} : 450 GeV - 7 TeV)

First measurement on \bar{p} from pHe (PRL2018) at $\sqrt{s_{NN}} = 110.5$ GeV. Data taken at 87 GeV, and recently with p, D and He at 70.9 and 113 GeV.

Methods developed to identify \bar{d} and \bar{He} .

LHC Run5 will allow nuclei identification.

- **ALICE**, has studied \bar{p} production pp, pPb, PbPb, XeXe, as well as \bar{d} , \bar{t} , ${}^3\bar{He}$, ${}^4\bar{He}$

Also data on coalescence processes.

LHC collider energies.

Main facilities and experiments for ongoing and future cross-section measurements - II

At the SPS:

- **AMBER** (successor of COMPASS). Has collected \bar{p} from collision of p with p , d , He , with total momentum between 10 GeV/c and 60 GeV/c, p_T up to 2 GeV/c.

\bar{p} from pHe measured at 6 energies between $\sqrt{s_{NN}}$ 10.7 and 21.7 GeV.

Isospin studies under way.

Improvement of spectrometer foreseen, increasing 10-100 read out rates.

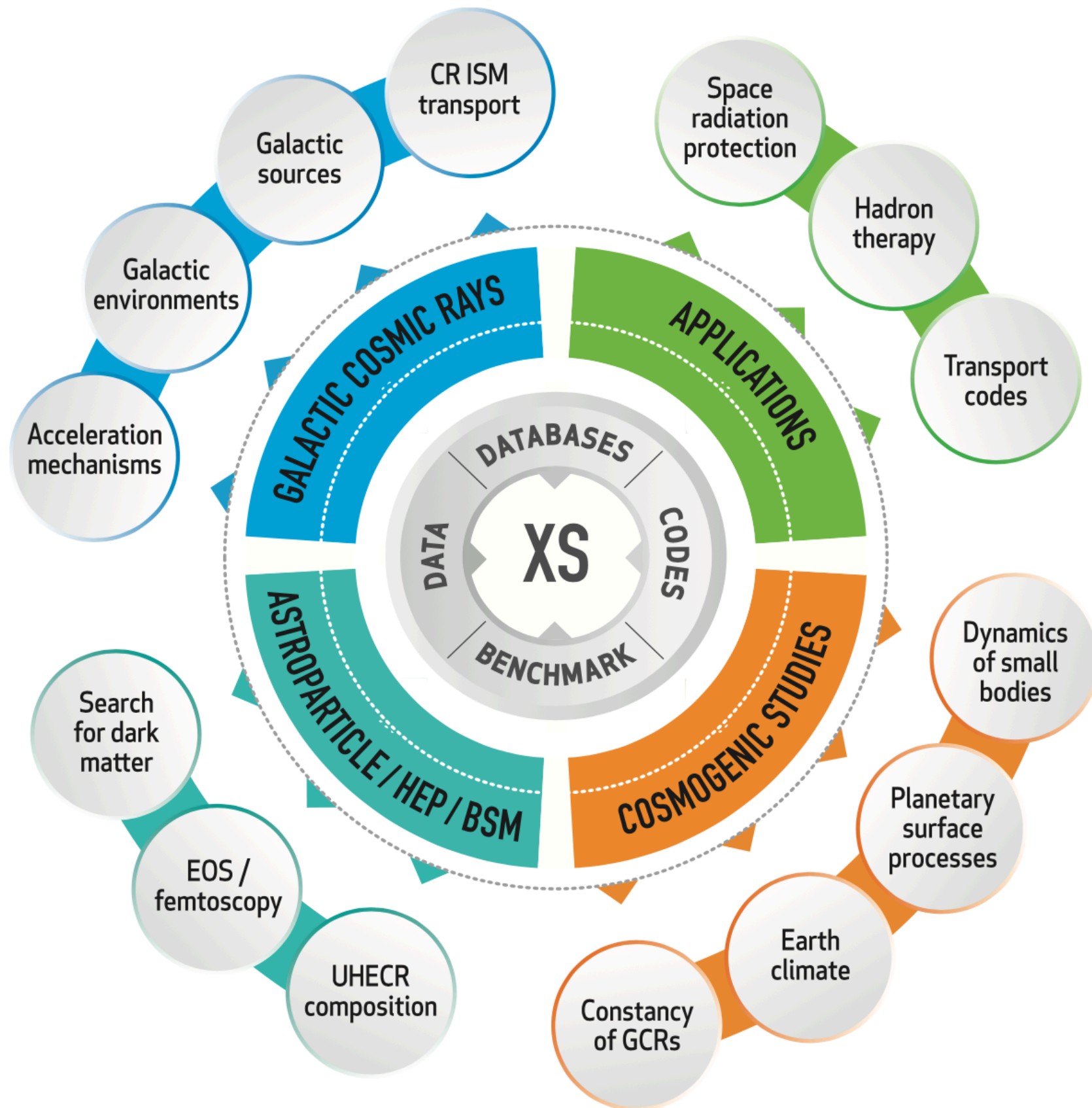
Identification of nuclei under study.

- **NA61/SHINE** (successor of NA49), hadron spectrometer.

Already recorded pp interactions with beam momenta 13-400 GeV/c, and pC , $\pi^{\pm}C$, $ArSc$, pPb , $BeBe$, $XeLa$ and $PbPb$ at different energies. They can measure \bar{p} , will \bar{d} .

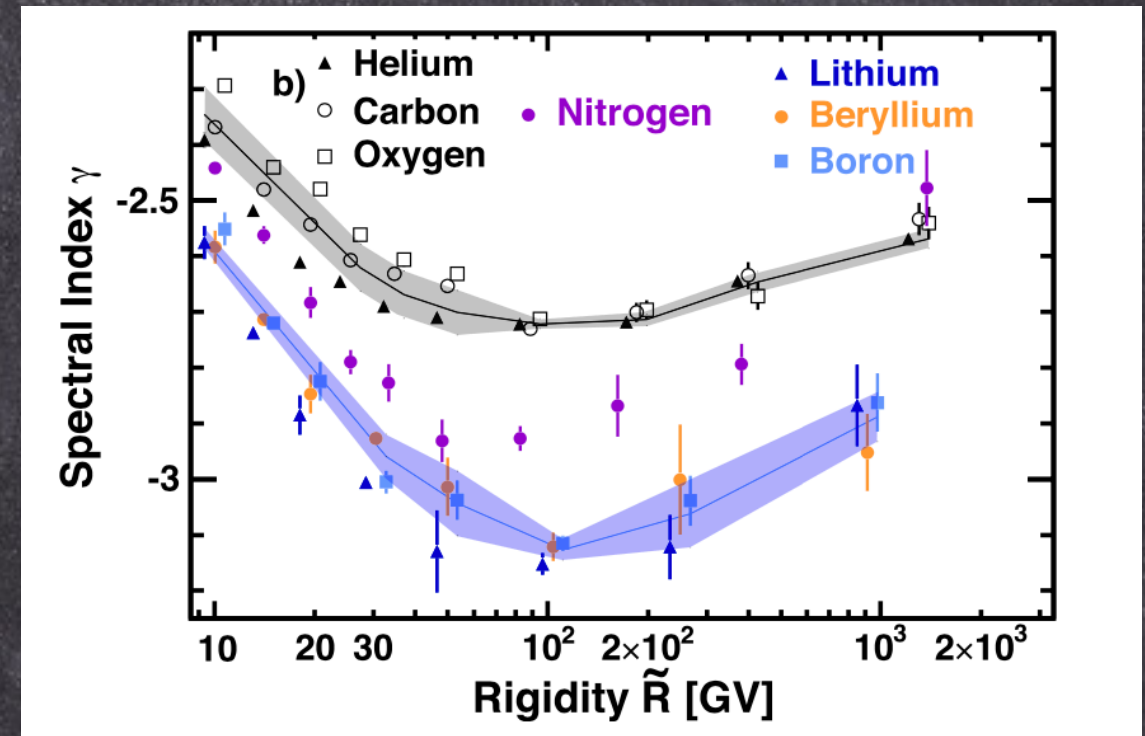
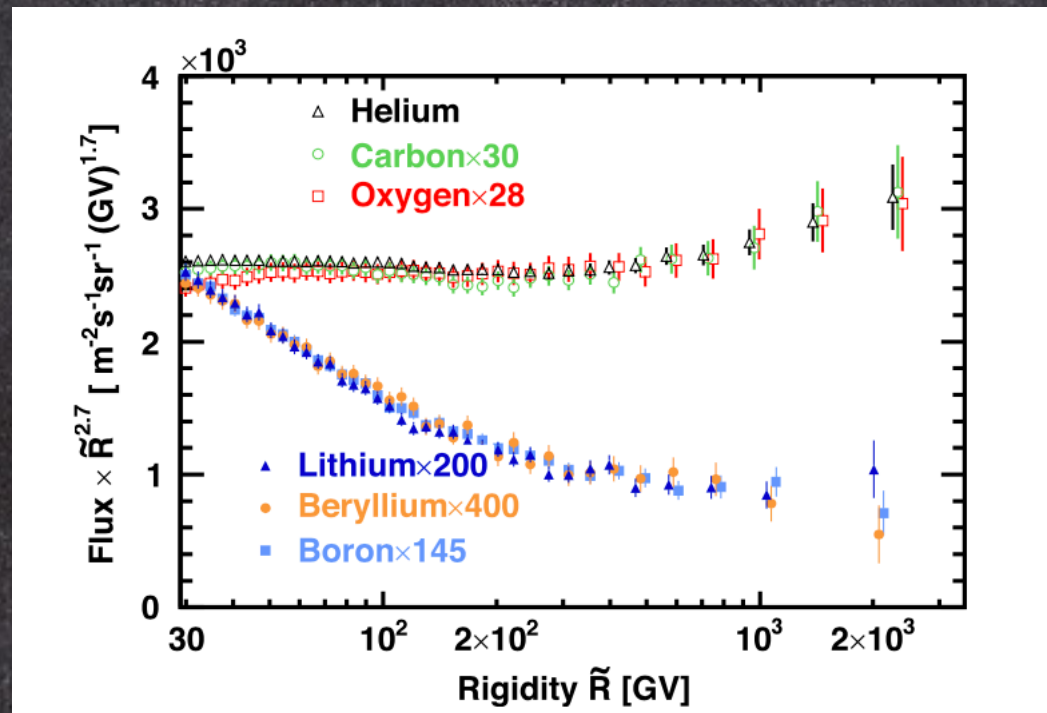
NA61/SHINE can measure nuclei fragmentation

More, but not applicable to Galactic cases: CERN n_TOF at 20 GeV from PS, RHIC, GSI, CNAO, HIAF, ..



Hardening of nuclear spectra

PAMELA Coll. Science 2011; AMS Coll Phys Rept 2021; PRL2017; PRL2018



A general hardening is observed at ~ 300 GV

The rigidity dependence of Li, Be and B measured by PAMELA and AMS are nearly identical, and different from the primary He, C and O (and also p).

The spectral index of secondaries hardens ~ 0.13 more than for primaries

Possible origin of anti-helium: anti-clouds, anti-stars

V. Poulin et al. PRD 2019

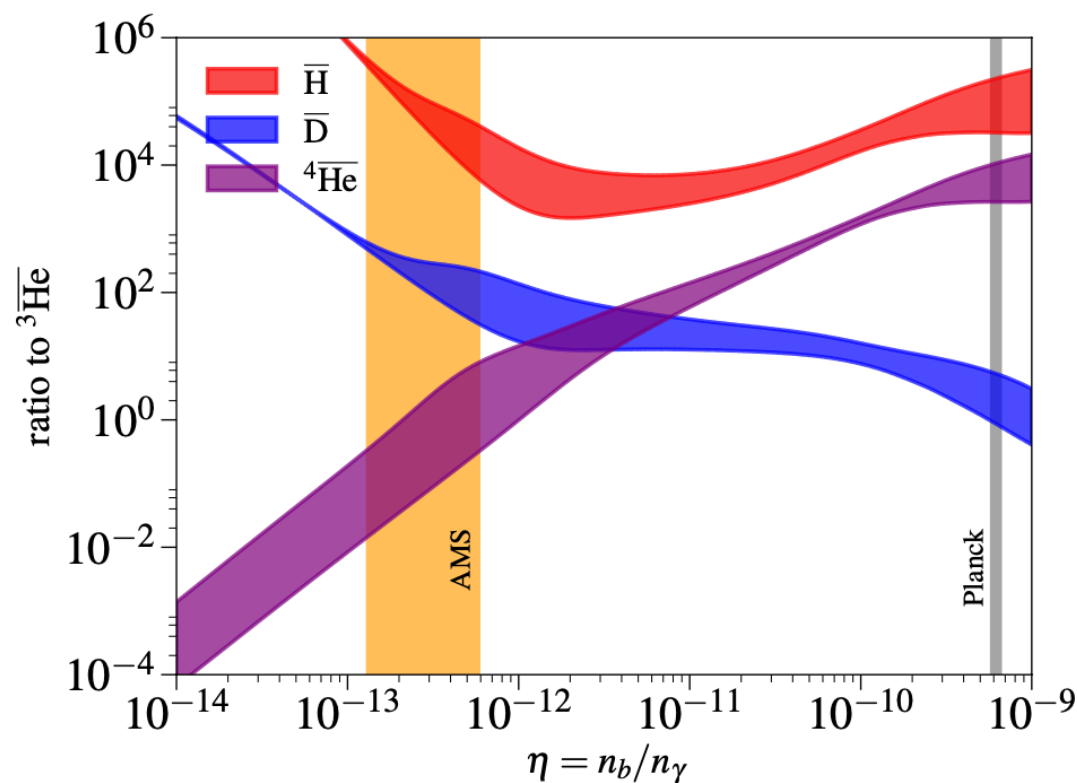


FIG. 4. Abundance of $\bar{\text{H}}$, $\bar{\text{D}}$ and $\bar{^4\text{He}}$ with respect to that of $\bar{^3\text{He}}$ as a function of the (anti-)baryon-to-photon ratio $\bar{\eta}$. The *Planck* value is represented by the grey band. The value required by the *AMS-02* experiment is shown by the orange band.

Anti-clouds: require anisotropic BBN
for the right $\bar{^3\text{He}}/\bar{^4\text{He}}$

AMS-02 measures are local, *Planck*'s
ones averaged over the Universe

Exotic mechanism for segregation of
anti-clouds is needed

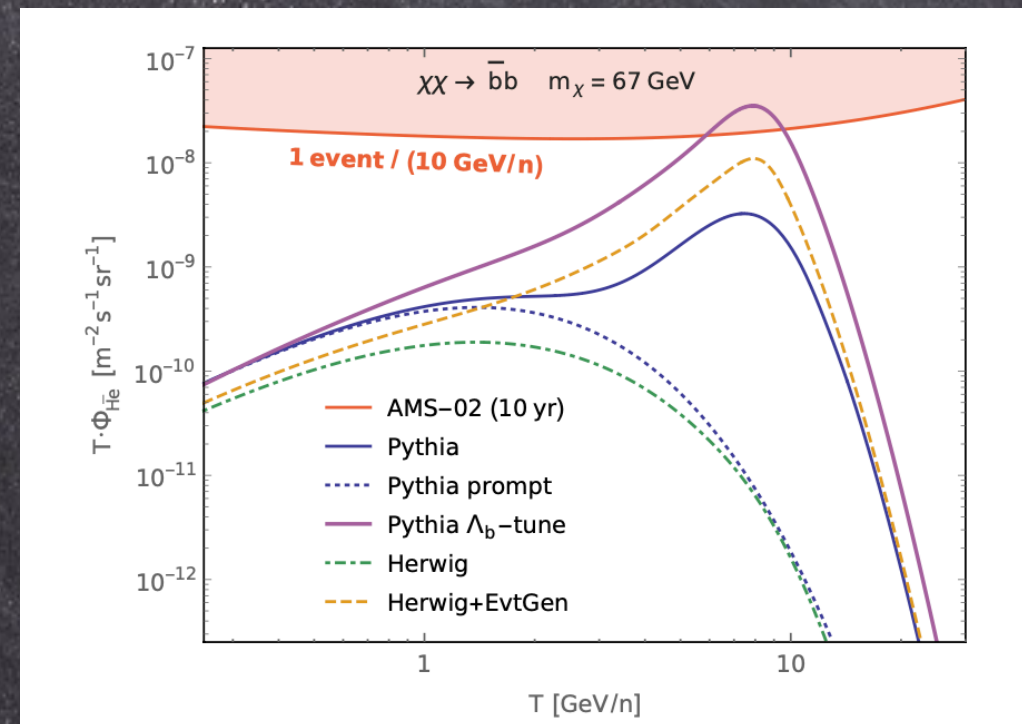
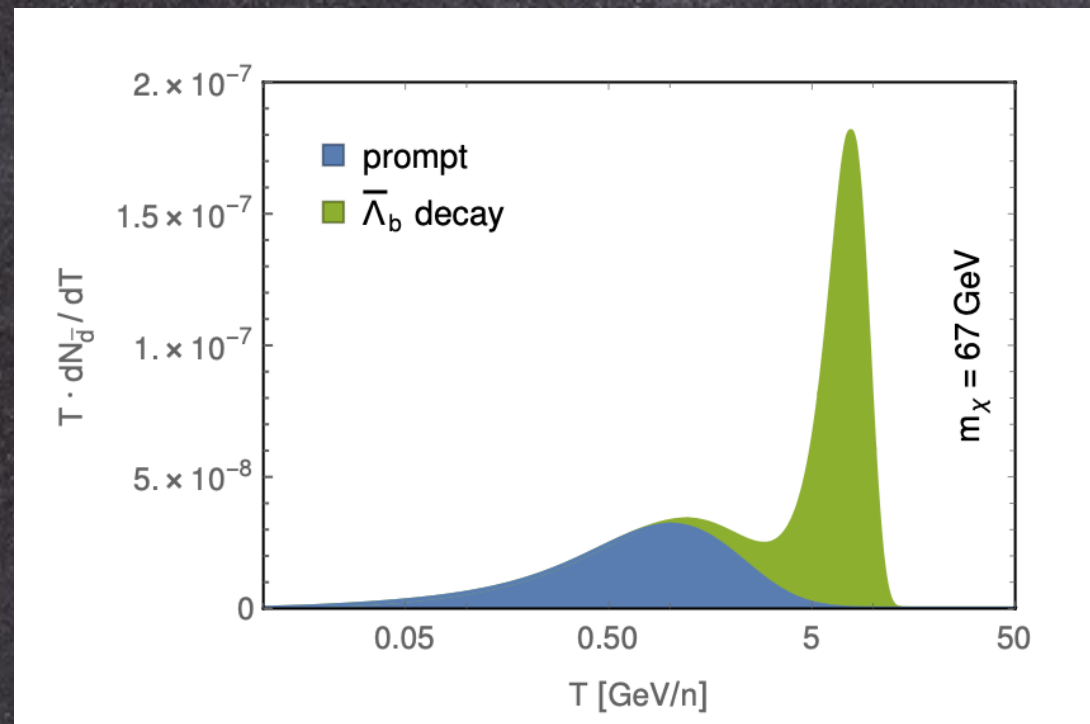
Traces in \bar{p} and $\bar{\text{D}}$

One anti-star could make the job.
How did they survive?

Enhancement of ${}^3\text{He}$ -bar production

Winkler & Linden PRL 2021

Consider the production of ${}^3\text{He}$ -bar through $\text{bar-}\Lambda_b$ (anti $u\bar{d}\bar{b}$) decays.

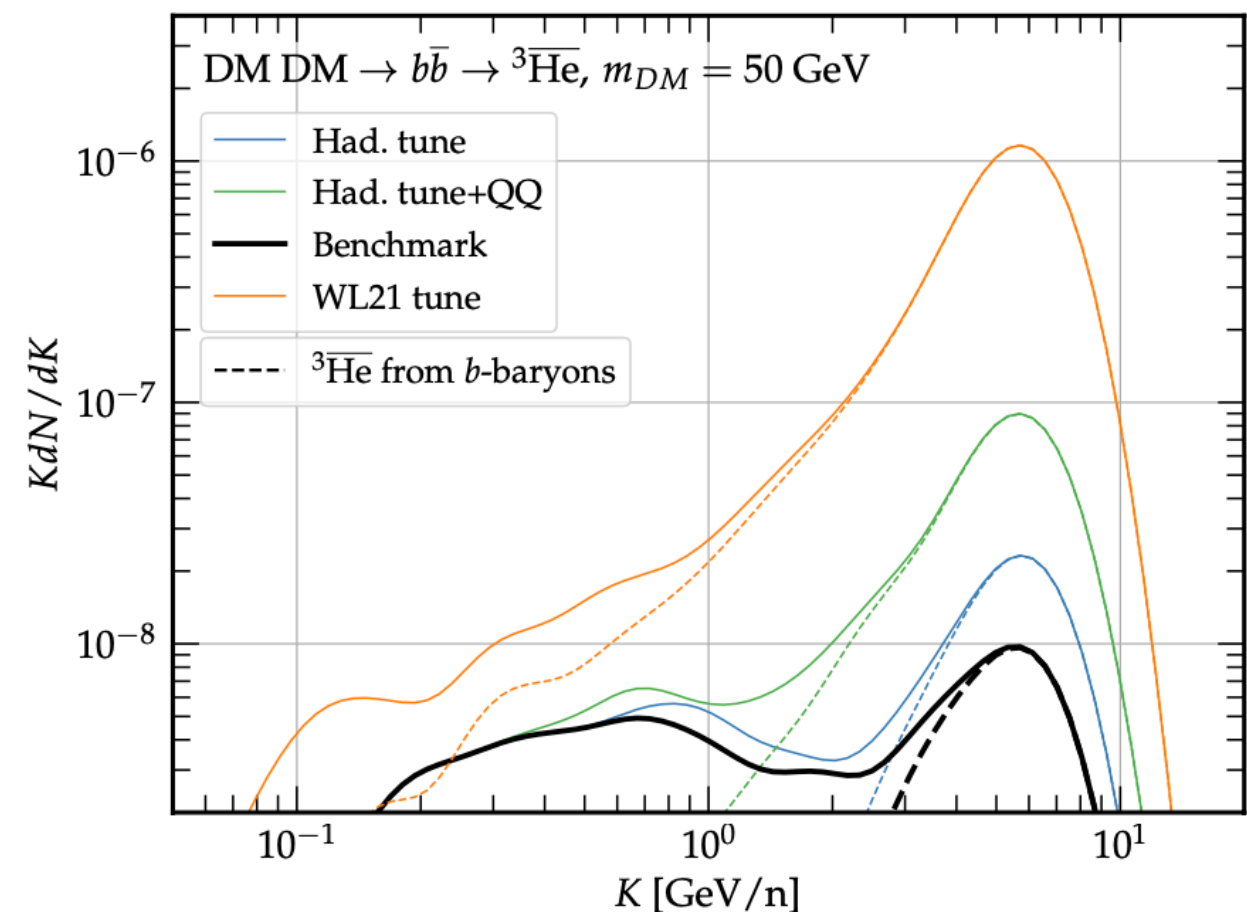
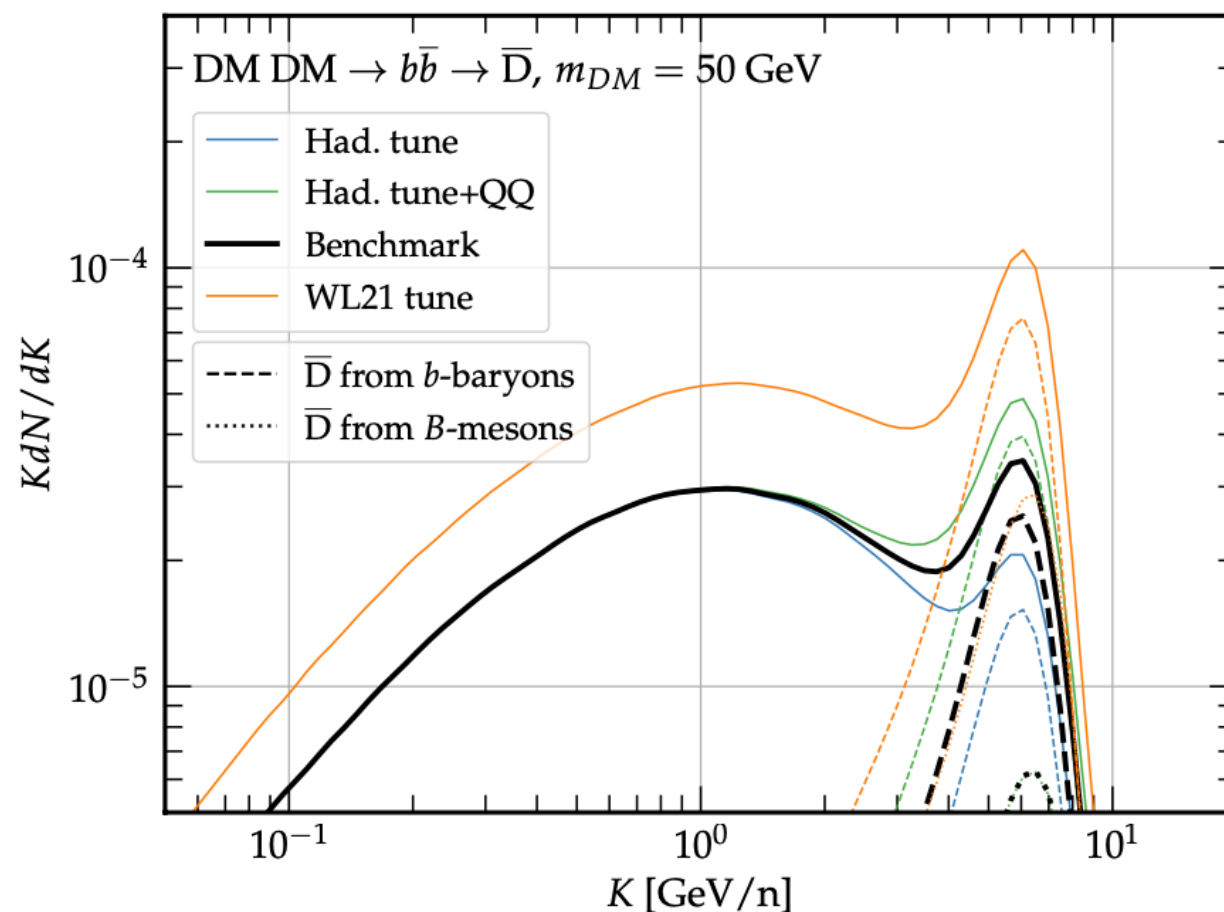


Production of anti-helium would be strikingly enhanced at few GeV.
Strong dependence on MC – Pythia, Herwig – tuning

Kachelrieß, Ostapchenko & Tjemsland 2105.00799 a strong criticism was raised:
The Pythia tune by WL21 affects all processes involving baryon and meson production

Implications from LHCb measurements

Di Mauro, Jueid, Köchler, Ruiz de Austri 2504.07172



LHCb sets strong upper bounds on Λ Branching ratios
Enhancement, if any, is very small